THESIS

CHEMICALLY MODIFIED CARRAGEENANS FOR MODULATING BIOLOGICAL RESPONSES: IMPACT OF CARBOXYMETHYLATION AND AMINATION ON ANTIOXIDANT, ANTIBACTERIAL, AND DEGRADATION PROPERTIES

Submitted by

Isaac Njoku

School of Biomedical and Chemical Engineering

In partial fulfilment of the requirements

For the Degree of Master of Science

Colorado State University

Fort Collins, Colorado

Spring 2026

Master's Committee:

Advisor: Matthew Kipper
Co-advisor: Ketul Popat

Melissa Reynolds
Margarita Herrera-Alonso
Megan Hill

ABSTRACT

CHEMICALLY MODIFIED CARRAGEENANS FOR MODULATING BIOLOGICAL RESPONSES: IMPACT OF CARBOXYMETHYLATION AND AMINATION ON ANTIOXIDANT, ANTIBACTERIAL, AND DEGRADATION PROPERTIES.

Carrageenans are sulfated polysaccharides derived from red seaweeds that have attracted significant attention for biomedical applications due to their biocompatibility, hydrophilicity, and structural tunability. Therefore, by chemically modifying their native forms we have more libraries of carrageenan derivatives with potential bioactivities in biomedical applications. This study focused on the chemical modification, characterization, and functional evaluation of three commercial types of carrageenan, kappa, iota, and lambda, to possibly alter their antioxidant, antibacterial, and degradation behavior, and to explore their application in layer-by-layer (LbL) polyelectrolyte multilayer (PEM) coatings.

Chemical modification was carried out through carboxymethylation and amination using several reaction routes, including Williamson ether synthesis, epichlorohydrin-based ring opening, and EDC/NHS and DMTMM coupling reactions. The structural modifications were confirmed by ^{1}H and ^{13}C NMR and FTIR spectroscopy, which revealed characteristic peaks corresponding to new carboxymethyl ($–CH_2COOH$) and amine ($–NH_2$) functional groups.

The antioxidant activities of the native and modified carrageenans were assessed using DPPH, ABTS, and FRAP assays. Results indicated a change in radical scavenging capacity for the modified samples. Antibacterial assays were performed against both Gram-positive (*Staphylococcus aureus*) and Gram-negative (*Pseudomonas aeruginosa*) bacteria using the broth

microdilution method. The modified carrageenans showed concentration and time dependent inhibition effects. All carrageenan and derivatives exhibited no notable inhibition against *P. aeruginosa*. These findings suggest that the chemical modification changes bacterial membrane interaction and surface binding through charge-based mechanisms.

To evaluate enzymatic degradation, both solution and surface studies were conducted using lysozyme as the enzyme at 0.01 mg/ml 0.25 mg/ml respectively. In solution, the reducing sugar generated was quantified using the p-hydroxybenzoic acid hydrazide (pHBH) assay, which confirmed changes over 10 days. Surface degradation of PEM coatings incubated in lysozyme for up to 21 days was characterized using atomic force microscopy (AFM) revealing changes of surface roughness over time.

Polyelectrolyte multilayers were formed using chitosan (CS) as the polycation and modified carrageenans as polyanions through the layer-by-layer (LbL) deposition method. A total of 16 alternating layers were deposited, terminating with the carrageenan derivative as the outermost layer. AFM revealed morphological differences between modified carrageenan PEMs and degraded PEMs.

Overall, this work demonstrates that chemical modification influences the functional versatility of carrageenans. Furthermore, their successful incorporation into PEM coatings shows strong potential for applications in biomedical surface engineering, such as antimicrobial coatings, wound dressings, and enzyme-responsive thin films.

ACKNOWLEDGMENTS

I am deeply grateful for the opportunity to pursue my graduate studies and research at Colorado State University. This journey has been a blessing, and I thank God for strength, guidance, and grace every step of the way.

My sincere appreciation goes to Prof. Matt Kipper. Thank you for your mentorship, patience, and support. You believed in me, challenged me, and always encouraged me to keep growing as a scientist and as a person. I am truly grateful to have had you as my advisor.

To my labmates and friends, thank you for your support, encouragement, and teamwork. Faith Lenell, thank you for your help in the lab and the long hours working side by side. Christian Fielding, thank you for your help with antioxidant studies. Mohammad Al Mesfer, thank you for being a supportive colleague and friend. To everyone in the Kipper lab, thank you for making this journey worthwhile and for the laughs and motivation along the way.

A special thank you to Dr. Liszt Yeltsin Madruga for guidance on carrageenan chemistries and for your support early in my research. I also appreciate Dr. Aniruddha Savargaonkar for assistance with bacterial studies, Dr. Rebeca Miller for help with XPS at ARC, and Dr. Michelle Mailhot for assistance with NMR.

To my family and loved ones, thank you for your endless prayers, love, and encouragement. Being far from home has not been easy, but your support kept me going. I am especially grateful to my parents and to everyone who believed in me even when the road was difficult.

Finally, I thank everyone who has been part of this journey, friends, colleagues, and community members. Your kindness and support made this experience meaningful and unforgettable.

TABLE OF CONTENTS

LIST OF FIGURES

1.0 Literature Review

1.1 Orthopedic Implants and the Role of Surface Coatings

Orthopedic implants are commonly used in modern medicine to support or replace damaged bones and joints (Seetharaman et al., 2023). These devices, which can be classified as permanent or temporary implants based on how long they are expected to stay in the human body, include hip and knee replacements, plates and screws for bone fixation, and other hardware like rods, pins, and bone cements. They are essential for restoring movement, relieving pain, and improving the quality of life in people who have suffered from injuries, fractures, arthritis, or other musculoskeletal problems (Jin & Chu, 2019).

The use of orthopedic implants continues to grow each year. The orthopedic implants market is projected to grow steadily, rising from about USD 26 billion in 2024 to roughly USD 32 billion by 2030. (*Orthopedic Implants Market Size | Industry Report, 2030*, n.d.) Ageing populations, obesity, increasing physical activity, and rising rates of joint and bone-related injuries are the main causes of this. (Mastnak et al., 2022) One of the treatments with the fastest rate of growth in the US is total hip arthroplasty (THA), which is expected to rise by 174% by 2030 (Gronbeck et al., 2020).The number of hip and knee replacements performed in the US is expected to increase by 2040 as more people live longer and stay active into old age. (Mastnak et al., 2022)

Although an implant's primary function is to offer physical support, its effectiveness frequently depends on how well it interacts with the body, its biocompatibility. The surface of the implant is the first area the body sees, and its behavior greatly influences whether the tissue around the implant heals correctly. (Fadzil et al., 2022). Unfortunately, many commonly used implants have smooth or inactive surfaces that do not encourage good bone interaction. In some cases, these

surfaces can even cause problems like inflammation or immune reactions, in which the body treats the implant like a foreign object (Supra & K Agrawal, 2023), infection, especially from bacteria that stick to the surface and form biofilms (Arciola et al., 2018a) and material breakdown, where the surface wears away or changes due to body fluids and movement (Yan et al., 2007).

These issues can lead to serious outcomes. For instance, implant-related infections affect about 1 to 2% of primary joint surgeries, and the numbers are much higher in revision cases ("Infection and Your Hip Replacement," n.d.; Zimmerli & Ochsner, 2003). Infections can delay healing, cause pain, and may even require the implant to be removed. Another common problem is aseptic loosening, where the implant becomes loose without any sign of infection. This is often caused by inflammation or poor bone growth around the implant (Ricciardi et al., 2025).

To reduce these risks, researchers and engineers are working to improve implant surfaces using special coatings (Mastnak et al., 2022). These surface coatings can be made from different types of materials—metals, ceramics, polymers, or combinations of them—and are designed to help the bone adhere to the implant better (osseointegration), to prevent bacteria from attaching to the surface, and to resist damage from the body's fluids, enzymes, or movement (Bohara & Suthakorn, 2022a).

Some coatings use materials like hydroxyapatite to mimic natural bone, while others use silver, copper or magnesium to kill bacteria (Bohara & Suthakorn, 2022b; Zhuang et al., 2021). There are also polymer-based coatings that act like soft layers to reduce inflammation or as reservoirs for drugs. However, not all coatings work well in every situation. Some metal-based coatings may cause toxicity, and synthetic polymers might not break down in a safe or controlled way (Mastnak et al., 2022). These concerns have increased the use of natural materials like biopolymers for implant coatings. These materials are often biocompatible, biodegradable, and can be chemically

modified to match different needs (Nathanael & Oh, 2020). In recent years, natural polysaccharides such as chitosan, alginate, hyaluronic acid, and others have been studied for this purpose. These materials can be tailored to resist infection, control degradation, and even support bone cell growth (Mastnak et al., 2022).

1.2 Infection and Biofilm Formation on Orthopedic Implants

Infection is one of the most serious complications associated with orthopedic implants (Villegas et al., 2023). Although modern surgical techniques and sterilization protocols have reduced the overall risk, implant-associated infections (IAIs) still occur in 1–2% of hip or knee replacements, and up to 4-5% in revision surgeries, especially in high-risk patients ("Infection and Your Hip Replacement," n.d.). These infections can be devastating, leading to pain, implant loosening, bone loss, and in severe cases, amputation or death. The emotional and financial costs to patients are high, and managing these infections puts a significant burden on healthcare systems (Schierholz & Beuth, 2001).

One of the key reasons why orthopedic implant infections are difficult to treat is the formation of bacterial biofilms. Once bacteria attach to an implant surface, they can secrete a sticky extracellular matrix that forms a protective barrier (Arciola et al., 2012). This structure, called a biofilm, shields the bacteria from antibiotics and immune cells. As a result, bacteria in a biofilm can survive antibiotic concentrations up to 1,000 times higher than free-floating (planktonic) bacteria. *Staphylococcus aureus, Pseudomonas aeruginosa* and *Escherichia coli* are common pathogens responsible for these infections (Arciola et al., 2018b). Among these, *Staphylococcus aureus* is especially dangerous due to its ability to rapidly form biofilms and produce toxins that damage surrounding tissue. Moreover, some strains have become resistant to multiple antibiotics, including

methicillin-resistant *Staphylococcus aureus* (MRSA), which makes treatment even more complicated (Zhuang et al., 2021).

The risk of infection is further increased by the fact that many implant surfaces are smooth, hydrophobic, and bioinert, which makes them excellent platforms for bacterial attachment. Once the bacteria settle, even a small number can trigger a chronic, low-grade infection that might not be detected immediately (Chae et al., 2020a). In such cases, patients may only begin to experience symptoms weeks or even months after surgery.

Currently, the standard treatment for implant-related infection involves a combination of aggressive antibiotic therapy, surgical debridement, and sometimes removal or replacement of the implant (Kunutsor et al., 2018). Unfortunately, these procedures are costly, invasive, and not always successful. Studies show that even after revision surgery, there is about 23% chance that the infection may return (Volpin et al., 2016).

To reduce the risk of infection, researchers have explored many surface treatment strategies for killing bacteria by introducing antimicrobial agents into coatings (Villegas et al., 2023; M. Wang & Tang, 2019).

Antibiotic-releasing coatings may lose their effectiveness over time or contribute to drug resistance. Metal-based coatings like silver or copper can be cytotoxic at high concentrations and may interfere with bone cell function. Furthermore, creating a surface that can both resist bacteria and support healthy bone growth remains a major challenge (Ahmadabadi et al., 2020).

As the need for safer, multifunctional coating grows, attention has turned to natural materials that are biocompatible, sustainable, and easy to modify. These materials are being engineered to resist bacterial colonization, prevent biofilm formation, and work in harmony with bone tissue (M. Wang & Tang, 2019).

1.3 Oxidative Stress and the Role of Antioxidant Functionality

In addition to infection, oxidative stress is another important factor that affects the long-term success of orthopedic implants. After implantation, the body initiates an inflammatory response, which includes the activation of immune cells like neutrophils and macrophages (Galliera et al., 2021a). These cells release reactive oxygen species (ROS) such as hydrogen peroxide (H_2O_2), superoxide (O_2^-), and hydroxyl radicals (•OH), which are part of the body's defense mechanism. While this response is helpful in killing bacteria and clearing debris, excessive ROS production can lead to oxidative stress — a condition where ROS levels overwhelm the body's natural antioxidant defenses (Hameister et al., 2020).

Oxidative stress near an implant site can damage surrounding cells and contribute to implant failure in several ways (Hameister et al., 2020). It can lead to protein oxidation, affecting signaling molecules and matrix proteins necessary for healing. It promotes lipid peroxidation, damaging cell membranes and triggering inflammation. Lastly, it can also cause DNA/RNA modification thereby damaging cells.

At the implant surface, oxidative stress may accelerate material degradation, especially in polymer-based coatings, leading to loss of function or the release of toxic degradation products. In metal implants, ROS can contribute to corrosion or ion release, which may trigger further inflammation or hypersensitivity reactions (Hameister et al., 2020).

In orthopedic patients, oxidative stress has been linked to delayed bone healing, poor integration of implants, and the development of chronic inflammatory conditions. This is particularly concerning in high-risk populations such as elderly patients, diabetics, or those with compromised immune systems, where the natural antioxidant defenses may already be weakened (Bădilă et al., 2022).

To reduce the impact of oxidative stress, researchers have been exploring ways to introduce antioxidant functionality into implant coatings (Yang et al., 2022). Antioxidants are molecules that neutralize ROS and help maintain a healthy balance between oxidative and reductive processes in tissues (Hameister et al., 2020). Some materials naturally contain antioxidant properties, while others can be chemically modified or combined with antioxidant agents to achieve this effect (Ahmad, 2021).

However, one of the main challenges is to develop coatings that can provide sustained antioxidant activity over time without interfering with other important surface functions, such as cell adhesion or bone integration. This has led to growing interest in natural and tunable coating materials that can combine antioxidant activity with other properties like biodegradability, antibacterial behavior, and structural stability (Vishnu et al., 2023). The various techniques for developing antioxidant coatings on implants include the layer-by-layer deposition of polyelectrolyte multilayers, immersion/dip coating, spin coating, plasma immersion ion implantation and plasma enhanced chemical vapor deposition.

1.4 Degradation and Surface Stability in Implant Coatings

Degradation is an important factor to consider in the design and selection of materials for orthopedic implants, especially for coatings that come into direct contact with the biological environment (M. Kumar et al., 2021). Whether a coating is intended to remain stable over the long term to prevent implant degradation or to gradually break down and resorb, its degradation behavior must be well understood and tightly controlled (Vahabzadeh et al., 2015).

In orthopedic applications, the degradation of polymeric implant coatings can occur due to a combination of chemical (hydrolysis), enzymatic, mechanical and oxidative processes. These processes are influenced by the surrounding pH, presence of enzymes, fluid flow, ROS levels, and

even the microbiological environment (Lyu & Untereker, 2009). If not properly managed, degradation can lead to loss of coating integrity, early failure, or release of by-products that may be harmful or trigger unwanted biological responses.

There are two broad classes of coatings used in orthopedics. Non-degradable (permanent) coatings are expected to maintain their structure and function throughout the lifespan of the implant. These are typically used on metallic implants like joint prostheses and are designed to improve biocompatibility or prevent infection. The second is biodegradable (resorbable) coatings, which are designed to break down gradually and are often used in temporary implants, fracture fixation systems, or tissue engineering scaffolds. Their degradation should ideally match the rate of tissue healing or remodeling (Lyu & Untereker, 2009).

For degradable coatings, the key challenge is achieving a predictable and uniform breakdown that does not compromise the mechanical performance of the implant or release toxic degradation products. Materials that degrade too quickly may leave the implant surface unprotected, while those that degrade too slowly may persist and trigger inflammation or fibrous encapsulation (Xia et al., 2025).

Researchers use several analytical techniques to evaluate and optimize degradation behavior. The choice of technique depends on the material being studied. Gel permeation chromatography (GPC) is used to monitor molecular weight changes of polymers (Tian et al., 2023). Atomic force microscopy (AFM) and ellipsometry are applied to observe changes in surface roughness and film thickness in both synthetic and biological materials (Castilla-Casadiego et al., 2018). X-ray photoelectron spectroscopy (XPS) detects chemical changes at the surface for a wide range of materials, including polymers, ceramics, and metals (Kravanja & Finšgar, 2021; Mitchell, 2020). Lastly, the pHBH (p-hydroxybenzoic acid hydrazide) reducing-sugar assay quantifies solution-

phase degradation in polysaccharide-based materials by tracking newly formed reducing ends, often reported as glucose equivalents (Vlcek et al., 2021).

Understanding how coatings behave over time in *in vitro* and *in vivo* environments is critical for ensuring their safety and effectiveness. Ideally, a surface coating should maintain its biofunctionality and integrity during the healing process, and if degradable, should do so in a controlled and predictable manner (Fischer et al., 2021).

In recent years, more attention has been given to the idea of "smart degradation" — designing materials that degrade in response to specific triggers such as pH changes, enzyme activity, or oxidative stress. This allows coatings to respond dynamically to the implant environment and release therapeutic agents or expose new functional groups at the right time (Joshi et al., 2023; Zhao et al., 2023).

Overall, achieving the right balance between stability and degradability is a key part of developing next-generation implant coatings. This balance becomes even more critical when coatings are expected to serve multiple roles, such as antibacterial protection, antioxidant delivery, and tissue integration support.

1.5 Design Strategies for Multifunctional Coatings: Material Platforms and Assembly Methods

As discussed in the previous sections, the success of orthopedic implants depends not only on their mechanical performance but also on how well they interact with the biological environment (Huzum et al., 2021; Lewallen et al., 2015). Implant failures often arise due to complications like bacterial infection, oxidative stress, and uncontrolled degradation. These challenges typically don't occur in isolation — they often overlap, especially during the early healing phase when inflammation, microbial invasion, and tissue remodeling are all taking place (Galliera et al., 2021b;

Inui et al., 2023). This reality has created a strong push toward developing multifunctional coatings that can tackle multiple biological issues at once.

An ideal implant coating for orthopedic use would prevent or limit bacterial colonization, reduce oxidative damage, exhibit controlled and predictable degradation, support bone healing and tissue integration and be biocompatible, non-toxic, and scalable for clinical translation. Meeting all these goals with a single material is not straightforward. As a result, researchers have developed a variety of smart design strategies and material systems that aim to combine multiple functionalities into a single, robust surface (Zhao et al., 2023).

1.5.1 Types of Surface Coating Strategies

Several surface engineering techniques have been explored in recent years to deliver active functionality to implant surfaces (Vishnu et al., 2023; Zhao et al., 2023). These include:

- Layer-by-layer (LbL) technique
- Immersion/dip coating
- Spin coating
- Plasma immersion ion implantation
- Plasma enhanced chemical vapor deposition

These approaches, especially layer by layer technique, offer the flexibility to integrate multiple functionalities into one coating — a key advantage over single-function materials (Zhao et al., 2023).

1.5.2 Natural Polymers as Bioactive Coating Materials

In parallel with these fabrication methods, the choice of coating material has shifted toward more biocompatible and sustainable options, especially those derived from natural sources (Kalpana Manivannan et al., 2024). Among these, natural polysaccharides have attracted significant

attention because of their low toxicity, structural similarity to extracellular matrix (ECM) components, chemical modifiability and potential to support cell attachment and healing.

Several polysaccharides have been used in orthopedic and other biomedical coatings (Kalpana Manivannan et al., 2024). Chitosan, a cationic polysaccharide derived from chitin, is known for its antibacterial properties and ability to promote wound healing. However, it is only soluble in acidic environments and can be unstable at physiological pH (Troy et al., 2021). Alginate is anionic heteropolysaccharide obtained from brown seaweed. Alginate is biocompatible and widely used in hydrogels and scaffolds but lacks strong cell adhesion and bioactivity without modification (Ahmad Raus et al., 2021). Hyaluronic acid is found naturally in connective tissues and it is excellent for promoting cell migration and wound healing, but has low mechanical strength and rapid degradation in vivo unless crosslinked (Yasin et al., 2022). Dextran and cellulose derivatives are useful in drug delivery and coatings, but they are limited by their lack of biological activity on their own (Pires et al., 2023). Carrageenan, a class of sulphated polysaccharides obtained from red algae, are biocompatible and possess bioactive properties like antibacterial, anticoagulant, and immunomodulation. (Pacheco-Quito et al., 2020).

1.5.3 Heparin: The Benchmark for Antithrombotic Coatings

Among natural polysaccharides, heparin stands out as one of the most extensively used materials in biomedical surface engineering, especially for antithrombotic and anti-inflammatory coatings. Its high negative charge and biological activity make it ideal for preventing blood clot formation and modulating immune responses (Zang et al., 2022).

However, despite its effectiveness, heparin has several limitations (Hedlund et al., 2013). It is animal-derived, usually from porcine or bovine sources, raising ethical, regulatory, and contamination concerns (Sargison et al., 2022). It is biologically unstable, and activity can vary

depending on the source and purification method. There is a risk of heparin-induced thrombocytopenia (HIT), a serious immune reaction that can lead to life-threatening clotting as patients are at risk of thromboembolism (Cuker et al., 2018). These issues have led researchers to seek heparin alternatives — materials that offer similar sulfated, bioactive properties, but are safer, more sustainable, and more chemically tunable.

1.6 The Shift Toward Heparin Substitutes

To address the challenges of using heparin, attention has turned to plant-based, sulfated polysaccharides that share similar chemical characteristics but offer better control over source, structure, and modification (Arlov et al., 2021; Madruga et al., 2025; Yao & Yim, 2021). These include, fucoidan (from brown algae), ulvan (from green algae) and carrageenan (from red algae). These marine polysaccharides often have sulfate groups, linear backbones, and functional group availability that make them attractive for surface modification and therapeutic use. Among them, carrageenan has emerged as one of the most promising due to its well-characterized chemical structure, multiple commercial types (kappa, iota, lambda) with different sulfate contents, film-forming ability and compatibility with LbL assembly and potential for chemical modification, allowing control over degradation, charge, and bioactivity (Pacheco-Quito et al., 2020).

1.6.1 Overview of Carrageenan

Carrageenan is a naturally occurring, sulfated high molecular weight polysaccharide extracted from red seaweeds (Rhodophyta), particularly species such as *Kappaphycus alvarezii* and *Eucheuma denticulatum* (L. Li et al., 2014; Rupert et al., 2022). It has been widely used in the food, pharmaceutical, and biomedical industries due to its gel-forming ability, biocompatibility, and hydrophilic nature. Structurally, carrageenan is composed of alternating 3-linked β-D-

galactopyranose and 4-linked α-D-galactopyranose units, which may be present in the 3,6-anhydro form and are variably sulfated depending on the type (L. Li et al., 2014).

The three major commercially important types of carrageenans as shown in scheme 1 include kappa carrageenan (KC) which contains one sulfate group per disaccharide and forms strong, rigid gels in the presence of potassium ions. Iota carrageenan (IC) has two sulfate groups per disaccharide and forms elastic, soft gels, especially with calcium. Lambda carrageenan (LC) contains three sulfate groups per disaccharide and does not gel, but forms highly viscous solutions.

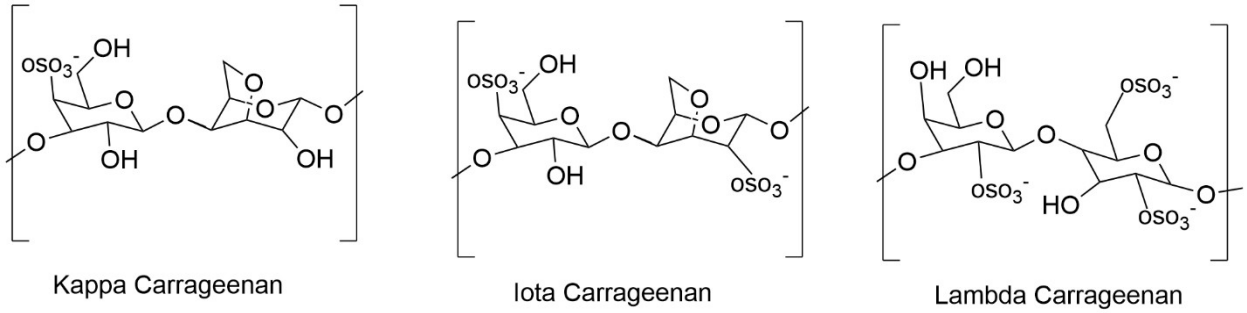

Scheme 1: Chemical structures of kappa, iota and lambda carrageenan backbone repeating units.

These structural differences significantly affect their rheological behavior, solubility, and bioactivity (Necas & Bartosikova, 2013). For instance, higher sulfate content generally correlates with stronger anticoagulant or antioxidant activity, but may also impact degradation rate and biostability (De Araújo et al., 2013; Humayun et al., 2023; Liang et al., 2014).

Carrageenan's natural origin, tunable sulfate content, and film-forming ability make it an attractive candidate for biomedical applications, particularly in the development of hydrogels, wound dressings, drug delivery systems, and surface coatings (Tavakoli et al., 2019; Yasin et al., 2022). Moreover, its structural resemblance to glycosaminoglycans (GAGs) like heparin adds further biomedical relevance, especially in the context of blood-compatible materials (Madruga et al., 2025; Song et al., 2018).

The structure of this wonder polysaccharide gives room for the introduction of new functionalities to it, thereby making it more biologically relevant. As a result, researchers have explored various chemical modification strategies to enhance its functionality and broaden its potential in tissue engineering and implant surface design (Mokhtari et al., 2021).

1.6.2 Biomedical Applications of Carrageenan

Carrageenan has attracted considerable interest in the biomedical field due to its biocompatibility, non-toxicity, and natural abundance (Pacheco-Quito et al., 2020). Its hydrophilic nature, structural similarity to glycosaminoglycans, and ability to interact with proteins and cells make it a useful material in a variety of applications (Kuznetsova et al., 2021). Over the past two decades, both native and modified carrageenans have been studied for roles in wound healing, drug delivery, tissue engineering, antiviral therapies, and biosensing (Neamtu et al., 2022; Setz et al., 2023; Žaimis et al., 2023).

In wound healing, carrageenan-based hydrogels have been used to maintain a moist environment, absorb exudates, and support cell migration. Studies have shown that incorporating sulfated polysaccharides, like carrageenan, into dressings can improve healing outcomes by modulating inflammation and stimulating angiogenesis (Neamtu et al., 2022).

In drug delivery systems, carrageenan has been used as a matrix or carrier for controlled release of therapeutics (Gupta, 2001). Its sulfate groups enable it to interact electrostatically with positively charged drugs, proteins, or nanoparticles, allowing sustained release and targeted delivery. For example, carrageenan-based microspheres and nanoparticles have been explored for oral, topical, and even injectable delivery routes, with good encapsulation efficiency and minimal cytotoxicity (C. Li et al., 2013).

In tissue engineering, carrageenan hydrogels and scaffolds have been studied as matrices for bone, cartilage, and skin regeneration (Yegappan et al., 2018). However, in their unmodified form, these materials often suffer from low mechanical strength and rapid degradation, which limits their standalone use in load-bearing or long-term applications. To address this, many studies have blended carrageenan with other polymers (e.g., gelatin, chitosan, PVA) or crosslinked it chemically to enhance stability (Loukelis et al., 2022).

These interesting applications of carrageenans have prompted increasing interest in chemical modification strategies to expand carrageenan's utility, particularly in applications requiring precise control over surface chemistry, degradation, and bioactivity.

1.6.3 Chemical Modifications of Carrageenan Reported in Literature

While native carrageenan possesses many desirable properties such as biocompatibility, film-forming ability, and sulfated functionality, its biological activity, mechanical properties, and degradation behavior are often insufficient for more demanding biomedical applications (Collén et al., 2009). As a result, a wide range of chemical modification strategies have been explored to enhance or tailor its performance. These modifications aim to introduce new functional groups, improve solubility, tune surface charge, adjust degradation rate, and enhance interactions with cells or microbes (Das & Bal, 2024; S. Kumar et al., 2025). Among the many strategies for polysaccharide modification, methacrylation, acetylation, phosphorylation, oxidation, thiolation, benzoylation, esterification, oversulfation, cationization and carboxymethylation are most of the commonly used methods employed for the chemical modification of carrageenan.

1.6.4 Limitations of Past Modification Strategies

While these chemical modifications have advanced carrageenan's performance in gels, hydrogels, and drug carriers, they often fall short when the material is applied as a surface coating, particularly

for blood-contacting or infection-prone applications (Das & Bal, 2024). Some limitations include use of harsh reagents or toxic crosslinkers, poor control over surface charge and film degradation rate and incompatibility with nanoscale assembly methods like layer-by-layer coating.

To address these challenges, researchers have increasingly focused on developing targeted, function-driven modification strategies that can introduce bioactive groups under mild, aqueous conditions, while remaining compatible with nanostructured surface assemblies.

1.6.5 Our Strategy

Since previous modifications have shown that the bioactivity of carrageenan can be altered through the incorporation of functional groups, we employed both carboxymethylation and amination routes to expand the library of available carrageenan derivatives and to understand their bioactivity at the nanoscale. Carboxymethyl groups were introduced into the three carrageenan types using the Williamson ether synthesis, resulting in derivatives denoted as CMKC, CMIC, and CMLC—representing carboxymethyl kappa-, iota-, and lambda-carrageenan, respectively. This reaction was carried out under basic conditions using NaOH solution, and monochloroacetic acid served as the carboxymethylating agent.

Our next strategy was to introduce amine functional groups into the native carrageenan backbone. To achieve this, we explored four amination routes: a nucleophilic substitution method, 1-ethyl-3-(3-dimethylaminopropyl)carbodiimide (EDC) coupling chemistry, 4-(4,6-dimethoxy-1,3,5-triazin-2-yl)-4-methylmorpholinium chloride (DMTMM) coupling chemistry, and epichlorohydrin–ammonium hydroxide (ECH–NH_4OH) chemistry. The sequence of these reactions followed the same order listed above. We attempted each chemistry in succession because the earlier methods, prior to the ECH–NH_4OH route, produced products that were unsatisfactory based on analyses using ^{1}H NMR, ^{13}C NMR, FTIR, and the 2,4,6-

trinitrobenzenesulfonic acid (TNBS) assay for amine quantification. The aminated products were designated as AKC, AIC, and ALC for aminated kappa-, iota-, and lambda-carrageenan, respectively.

In the nucleophilic substitution method, 2-chloroethylamine hydrochloride (2-CEA) was used as the aminating agent, replacing monochloroacetic acid used in the carboxymethylation step. EDC and DMTMM are well-documented coupling agents for introducing amine groups into polysaccharides, and both were applied using the carboxymethylated carrageenans as substrates, which provided the required carboxyl groups. These reactions proceed through the formation of reactive intermediates that can be attacked by an aminating agent—in this case, ethylenediamine (EDA)—to yield aminated products. EDC reaction was carried out in MES buffer (pH 4.5) and the DMTMM reaction in deionized (DI) water.

However, limitations such as undetectable amine content in the TNBS assay and the likelihood of ionic bonding between the amine and carrageenan prompted us to explore alternative amination routes. This led us to investigate the ECH–NH_4OH method, previously reported for the amination of fucoidan (J. Wang et al., 2009). This chemistry introduces amine groups by first forming an epoxide intermediate with epichlorohydrin, which is subsequently opened by ammonium hydroxide. Using this method, all analyses confirmed successful amination of kappa- and lambda-carrageenans. For iota-carrageenan, however, an insoluble product was obtained, likely due to crosslinking and gelation observed during the reaction.

1.6.6 Justification for Chosen Modifications

The chemical modifications used in this study—carboxymethylation and amination—were chosen carefully with the goal of making carrageenan more suitable for biomedical surface applications, especially as a potential substitute for heparin (Madruga et al., 2025; Song et al., 2018).

Carrageenan shares some structural similarity with heparin, particularly in its linear backbone and negatively charged sulfate groups. This makes it a promising alternative, especially because it is plant-based, more sustainable, and easier to source (Song et al., 2018). However, in its native form, carrageenan does not have all the properties needed for use in advanced biomedical coatings.

To improve these limitations, two modifications were introduced. The first was carboxymethylation, which adds carboxyl (-COOH) groups to the carrageenan chain (Leong et al., 2011). This increases the negative charge on the molecule, bringing it closer to the charge density of heparin. In addition, carboxyl groups are known to have mild antioxidant properties, which can help reduce oxidative stress in the body—a common problem around implants (Madruga et al., 2020). Carboxymethylation also improves the solubility and hydrophilicity of the polymer, making it easier to work within coating applications and layer-by-layer assembly.

The second modification was amination, where primary amine ($-NH_2$) groups were introduced onto the polysaccharide (Dedhia et al., 2021; Labafzadeh et al., 2015). Here, we introduce a carrageenan amination route that, to our knowledge, is novel for carrageenan and was adapted from an epichlorohydrin–ammonium hydroxide reaction previously applied to laminaran and fucoidan (Malyarenko et al., 2020; J. Wang et al., 2009).

This amination method introduces protonatable amine groups into carrageenan, which can provide localized positive charges under physiological conditions (Fatima et al., 2023). Although heparin also contains glucosamine units, its amines are primarily N-sulfated or N-acetylated and therefore not present as free primary amines. In contrast, aminated carrageenan introduces accessible amine groups that contribute localized cationic character and enable electrostatic assembly. As a result, introducing amine groups enables us to tune the ratio of positively charged to negatively charged groups in the polymer chain, thereby changing electrostatic interactions that regulate biomolecule

interactions and electrostatic self-assembly. Furthermore, these polymers, when interacting with polycations like chitosan, can be used to form coatings that allow for fine control over thickness, degradation, and surface properties. Beyond these physical properties, amine groups in polysaccharides have been reported to be powerful in targeting cancer cells (Malyarenko et al., 2020).

Overall, both modifications were chosen to not only mimic some of the key properties of heparinlike its charge and protein-binding ability, but also to go a step further by giving carrageenan new, improved properties such as antibacterial behavior, antioxidant potential, and tunable degradation. They also allow the material to be used in nanoscale coating systems, which are increasingly important for next-generation biomedical implants. These modifications were done under mild, water-based conditions, reducing the use of harsh or toxic chemistries.

1.6.7 Relevance to Surface Coating Applications

The motivation for modifying carrageenan in this work was not only to improve its intrinsic properties, but to make it a viable material for surface coating applications in the biomedical field (Zhuikova et al., 2020). As discussed earlier, the surface of an implant plays a major role in determining how the surrounding tissue responds to it. In orthopedic implants, problems like bacterial infection, oxidative stress, and uncontrolled degradation are common and often lead to implant failure (Esquivel-Chirino et al., 2021). Therefore, developing a coating system that could address these challenges using natural, tunable, and scalable material is of importance.

The modified carrageenans, were used in this work to form polyelectrolyte multilayers (PEMs) (Boddohi et al., 2010) based on electrostatic interactions between positively charged polymers (chitosan) and negatively charged carrageenan derivatives.

The PEMs were built using a LbL method, where alternating layers of anionic carrageenan derivatives and cationic chitosan were deposited on a substrate. This technique allowed for precise control over the thickness and composition of the coating. It also made it possible to tune the surface charge, roughness, and degradation behavior simply by adjusting the number of layers or the type of carrageenan used (Izumrudov et al., 2018). These coatings were evaluated using surface analysis tools such as X-ray photoelectron spectroscopy (XPS), and water contact angle measurement (Almodóvar et al., 2011).

Altogether, surface modifications demonstrate how simple, targeted modifications to a natural polymer can lead to versatile and multifunctional materials that meet the demands of modern implant coatings. They offer a balance between biocompatibility, bioactivity, and processability, while also being plant-derived and scalable. The combination of chemical tunability, surface adaptability, and biological function makes modified carrageenan a strong candidate for next-generation orthopedic implant coatings, especially in settings where a heparin substitute is desired.

2.0 Thesis Aim Overview

Despite widespread research on natural polysaccharides as functional biomaterials, chemically modified carrageenans remain significantly underexplored, particularly in the context of surface engineering and biological response. Carrageenans—sulfated galactans derived from red seaweed—are known for their biocompatibility, biodegradability, and diverse chemical structure. However, their utility is often limited by insufficient charge density, or lack of functional handles for conjugation. While carboxymethylation and amination have been used to improve other polysaccharides, there is limited knowledge on how these modifications affect carrageenan's antioxidant, antimicrobial, and enzymatic degradation behavior, especially across its kappa, iota, and lambda variants.

Furthermore, although layer-by-layer (LbL) assembly of polyelectrolyte multilayers (PEMs) has shown promise in surface coating applications, there are no detailed studies evaluating how the chemical structure of modified carrageenans influences PEM formation, stability, or surface characteristics. This gap limits our ability to rationally design carrageenan-based coatings for medical devices, tissue scaffolds, or wound healing materials.

In this work, chemical modification of kappa (KC), iota (IC), and lambda (LC) carrageenans will be carried out in order to investigate how their functional group composition affects antioxidant behavior, antibacterial activity, enzymatic degradability, and polyelectrolyte multilayer assembly. The goal is to establish structure–function relationships that can guide the design of carrageenan-based biomaterials with tunable bioactivity.

2.1 Overall Goal and Specific Aims

The overall goal of this work is to design and synthesize chemically modified carrageenans capable of modulating biological responses through structural and surface-level functionalization. By introducing carboxymethyl and amine functional groups into kappa, iota, and lambda carrageenans, this research seeks to expand the library of bioactive polysaccharides and elucidate how these chemical modifications influence nanoscale interactions and biological activity.

To achieve this goal, the following specific aims were established:

1. Synthesize chemically modified carrageenans

Each of the three carrageenan types (KC, IC, and LC) will be chemically modified via (a) carboxymethylation and (b) several amination routes, including nucleophilic substitution, epichlorohydrin-based ring opening, and carbodiimide (EDC/NHS or DMTMM) coupling. These reactions are intended to increase functional group availability and charge density, thereby enhancing water solubility, binding capability, and biological reactivity.

2. Evaluate biological and degradation properties of modified carrageenan.

The antioxidant performance of native and modified carrageenans will be assessed using multiple radical scavenging assays (DPPH, ABTS, and FRAP), while antibacterial activity will be evaluated against both Gram-positive and Gram-negative bacterial strains using broth microdilution and growth inhibition assays.

3. Develop and characterize polyelectrolyte multilayer (PEM) coatings using the layer-by-layer technique.

Using chitosan as polycation, modified carrageenans will be assembled into 16-layer PEMs via the layer by layer (LbL) method. The effect of modification on layer growth, thickness, and surface morphology will be studied using ellipsometry and atomic force microscopy.

3.0 Methods

3.1 Materials and Instrumentation

Kappa, iota, and lambda carrageenan were obtained from Thermo Fisher Scientific. Lambda carrageenan was further purified by dialysis against water. According to the supplier, the polymers' average molecular weights ranged from 400 to 788.647 g/mol.

Reagents used for antioxidant assays included 2,2-diphenyl-1-picrylhydrazyl (DPPH, ≥95%), 2,4,6-tripyridyl-s-triazine (TPTZ, ≥98%), ferric chloride hexahydrate (≥98%), 2,2′-azino-bis(3-ethylbenzothiazoline-6-sulfonic acid) diammonium salt (ABTS, ≥98%), potassium persulfate (≥99%), and Trolox (≥97%), all purchased from Sigma-Aldrich. Lysozyme (from chicken egg white, ≥95% protein, lyophilized powder) was also obtained from Sigma-Aldrich. Deionized water was used in all experiments.

^{1}H and ^{13}C NMR spectra were collected on a Bruker NEO400 spectrometer operating at 400 MHz using D_2O as solvent. An ATR-FTIR on the PerkinElmer Spotlight 400 FTIR Microscope and an XPHI Physical Electronics PE-5800 X-ray Photoelectron Spectrometer (XPS) were used. Static contact angle measurements for surface wettability were performed with a Ramé-Hart goniometer. Antioxidant and antibacterial absorbance measurements were collected using a FLUOstar Omega microplate reader.

Data were processed and analyzed using MNOVA for NMR, and CASAXPS for XPS**.** Excel and Python (Pandas, NumPy, SciPy, Statsmodels, and Matplotlib) were used for antioxidant and antibacterial assay data. Statistical significance was determined using one-way ANOVA followed by Tukey's HSD post hoc test ($p < 0.05$). Calibration curves for degradation experiment data were generated with four-parameter logistic (4PL) curves fitting in Python.

3.1 Chemical Modification of Carrageenan

3.1.1 Carboxymethylation

The Williamson ether method, previously utilized for carrageenan carboxymethylation, was adapted with minor modifications for the carboxymethylation of lambda carrageenan (Madruga et al., 2020). To begin, we purified 2 g of lambda carrageenan (LC) by dissolving it in 200 ml of deionized (DI) water overnight. The resulting solution was dialyzed against water for 3 days with frequent changes. After dialysis, the purified LC was frozen at -80 °C and then freeze-dried using a lyophilizer. Next, 1g of purified LC was suspended in 20 ml of 80% aqueous isopropanol for 30 minutes at 40 °C with vigorous stirring in a 50 ml, two-necked round-bottom flask fitted with a reflux condenser. After that, 2 ml of 20% NaOH was added dropwise over 15 minutes, and the mixture was stirred for 1 hour. During this period, the etherification solution was prepared by stirring 0.875 g monochloroacetic acid (MCA) in 2 ml of 20% aqueous NaOH for at least 20 minutes. The prepared MCA solution was then added dropwise to the reaction mixture over 20 minutes, followed by stirring at 55 °C for 4 hours. The carboxymethylated lambda carrageenan (CMLC) was vacuum filtered, washed three times each with 100 ml of 80% and then 100% aqueous isopropanol, dissolved in DI water overnight, dialyzed for 3 days, frozen at -80 °C, and lyophilized. This procedure was also applied for the carboxymethyl kappa (as shown in scheme 1) and iota carrageenan but without purifying them prior to carboxymethylation.

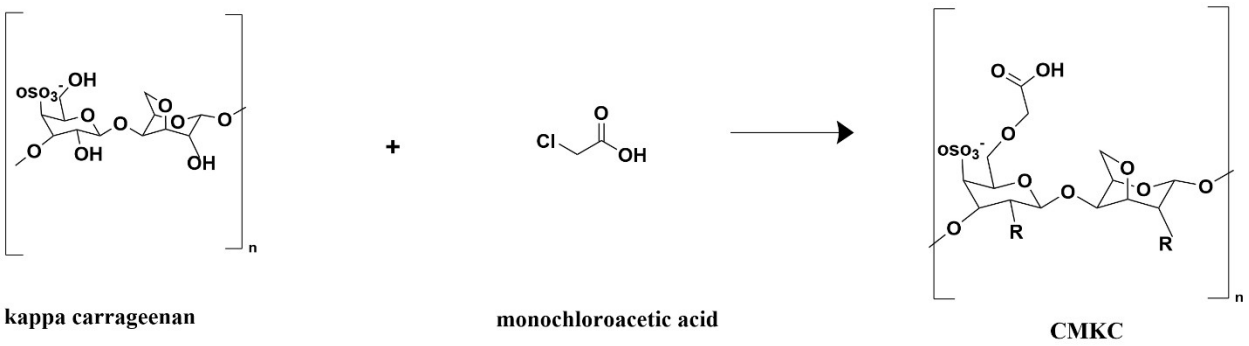

Scheme 2: Carboxymethylation of carrageenan using the Williamson ether synthesis.

3.1.2 Amination of Carrageenan

Amination of carrageenan is a novel process, and to the best of our knowledge, it has not been previously described in the literature. This modification introduces amine groups into the polysaccharide. To achieve this, we attempted several distinct amination procedures, including nucleophilic substitution, followed by amidation with ethylenediamine and ring-opening ether formation using epichlorohydrin followed by ammonium hydroxide treatment. For each of the amination routes, kappa carrageenan or its carboxymethylated derivative (CMKC) was first used, and if the chemistry was successful, it was then applied to aminate iota and lambda carrageenan.

3.1.2.1 Nucleophilic Substitution Method

This reaction followed a similar procedure used for the carboxymethylation of carrageenan (Dedhia et al., 2021; Madruga et al., 2020). However, 2-chloroethylamine (2-CEA) was used as the aminating agent for the possible introduction of the amine group in the place of monochloroacetic acid (MCA) used for carboxymethylation as shown in Scheme 3.

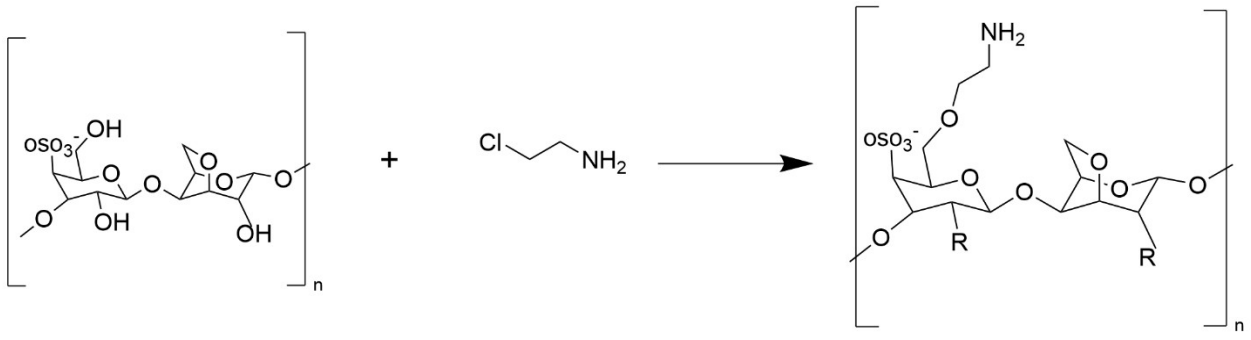

Scheme 3: Nucleophilic substitution method for the amination of kappa carrageenan.

3.1.2.2 Amidation of Carboxymethylated Carrageenan using Ethylenediamine

Two different carbodiimide coupling agents, 1-ethyl-3-(3-dimethylaminopropyl)carbodiimide (EDC) and 4-(4,6-dimethoxy-1,3,5-triazin-2-yl)-4-methylmorpholinium chloride (DMTMM), were used as activating agents for the possible amination of carboxymethylated kappa carrageenan (CMKC) with ethylenediamine (EDA) (D'Este et al., 2014). For each coupling reaction, the combined molar ratio of CMKC, EDC and EDA was 1:2:3 respectively. Briefly for EDC coupling reaction as shown in scheme 4., 0.5 g of CMKC was dissolved in 100 ml of 2-(*N*-morpholino)ethanesulfonic acid (MES) buffer (pH 4.5) overnight. Then, 192 mg EDC was added and reacted for 30 minutes. The pH was then adjusted to 8 using 0.1 M NaOH, followed by dropwise addition of 205 µL EDA. The amination reaction was allowed to proceed for 3 hours while stirring at room temperature. The final product was then dialyzed against water for 3 days, frozen at -80 °C and lyophilized. A similar procedure was followed using DMTMM coupling reaction. Here, 250 mg of CMKC was dissolved in 50 ml of DI water overnight and then 143 mg of DMTMM was added to the solution and the reaction was allowed to proceed for 30 minutes. The aminating step proceeded for 5 hours at room temperature by adding 103 µL of EDA to the

reaction mixture and similar post reaction steps used for EDC were employed to this reaction product. Scheme 5 shows the DMTMM coupling reaction chemistry.

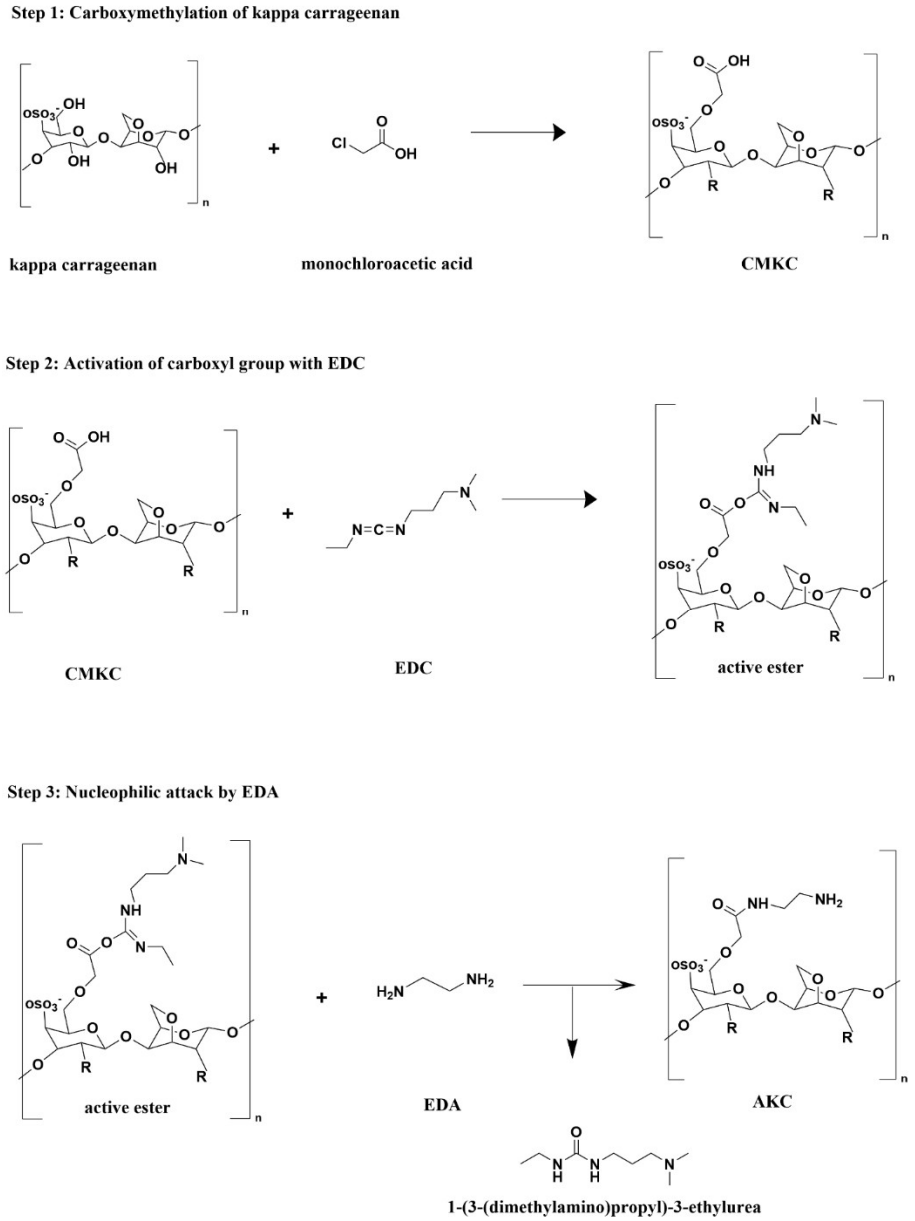

Scheme 4: EDC coupling chemistry for the amination of kappa carrageenan.

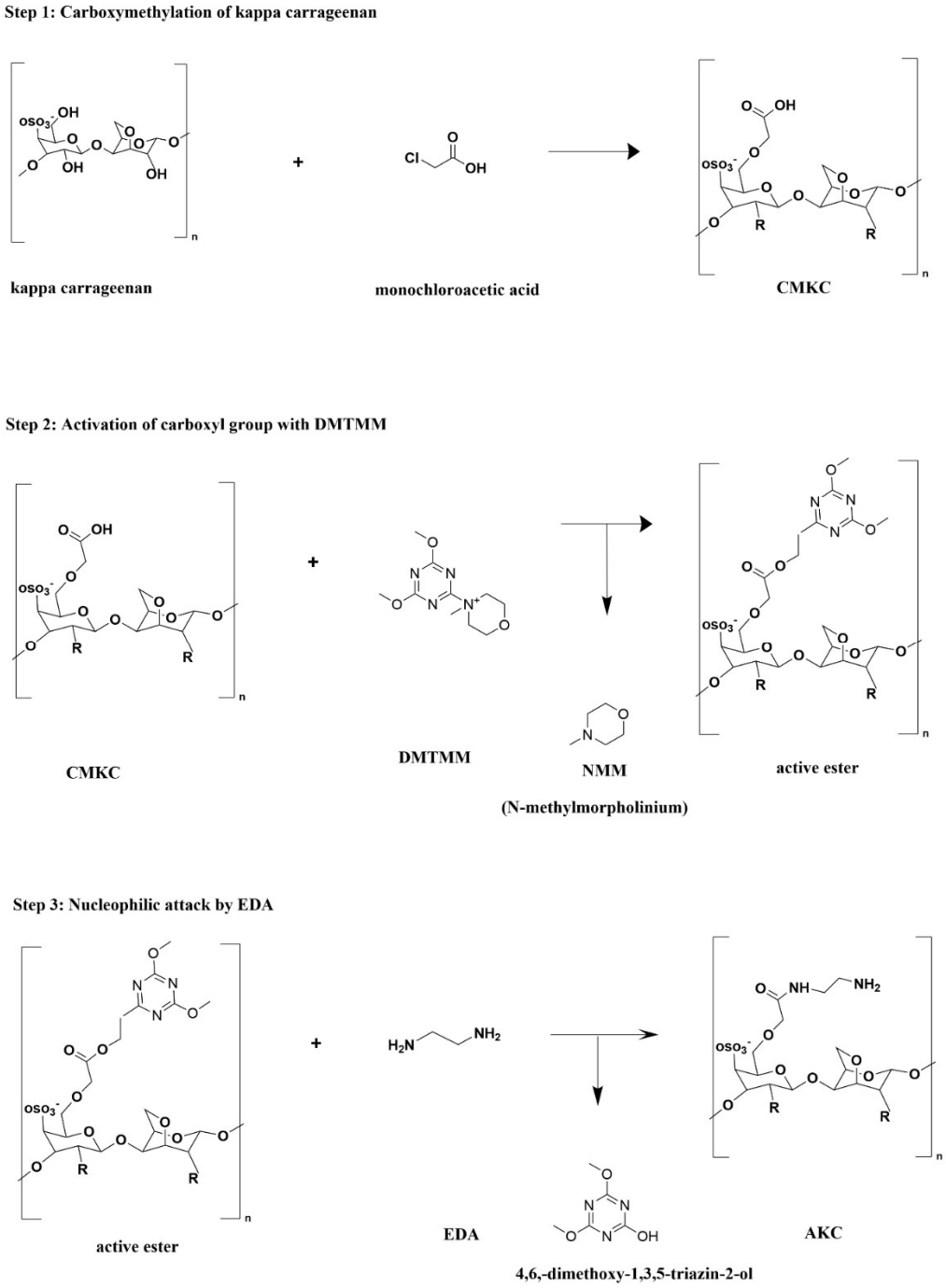

Scheme 5: DMTMM coupling chemistry for the amination of kappa carrageenan.

3.1.2.3 Epichlorohydrin-Ammonium Hydroxide Chemistry.

The procedure previously used for the amination of laminaran and fucoidan was adapted here with slight modifications (Malyarenko et al., 2020; Soeda et al., 1994). Specifically, 1 g of KC was dissolved overnight in 100 mL of DI water at room temperature. After dissolution, 10 ml of 2.6 M NaOH was added dropwise over 30 minutes, and the reaction mixture was stirred for 2 hours. Next, 6 mL of epichlorohydrin was added, and the reaction continued for an additional 2 hours. Afterward, the product was dialyzed against water for 3 hours. The pH of the dialyzed product was then adjusted to 11.5, and it was reacted with 20 ml of 25% ammonium hydroxide for 4 hours at 40 °C. The final product was dialyzed sequentially against 4.5 mg/mL $MgCl_2$, 5 mg/mL NaCl, and water, with the $MgCl_2$ and NaCl steps repeated three times at 12-hour intervals. This reaction is shown in scheme 6.

A similar method was used for the amination of lambda carrageenan. First, 1 g of LC was dissolved in 100 mL of water and purified by dialysis. The dialysate was then reacted with 10 mL of 2.6 M NaOH at 40 °C for 30 minutes, followed by the addition of 12 mL of epichlorohydrin (99.8% purity) for 2 hours.

Without dialysis of the product, the pH of the mixture was adjusted to 10.5. Then, 40 ml of 25% ammonium hydroxide was added, and the mixture was stirred for 8 hours at 40 °C. The final product was dialyzed sequentially against 4.5 mg/ml magnesium chloride, 5 mg/ml NaCl, and water, with each dialysis step repeated three times at 12-hour intervals.

The epichlorohydrin-ammonium hydroxide procedure used for kappa- and lambda-carrageenan was attempted for the animation of iota carrageenan.

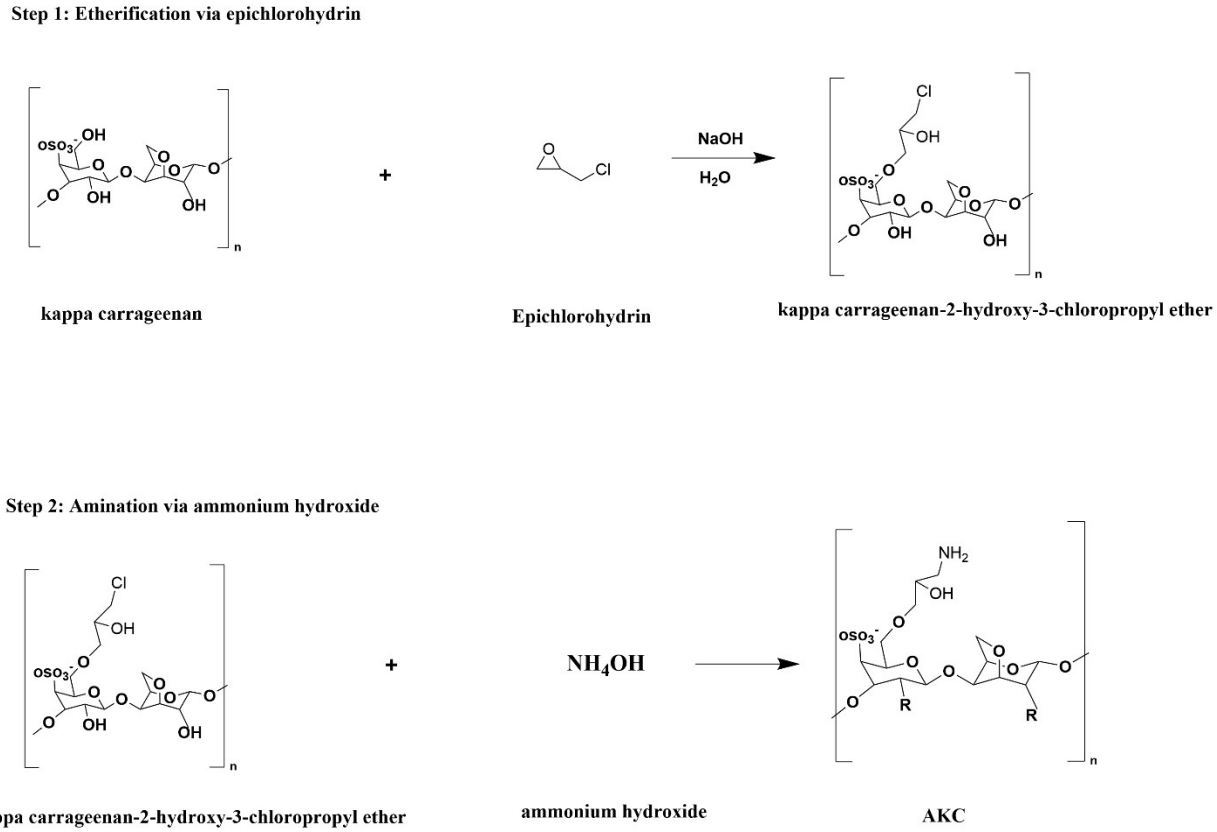

Scheme 6: Epichlorohydrin-ammonium hydroxide chemistry for the amination of kappa carrageenan.

3.2.1 Polyelectrolyte Multilayer (PEM) Formation with Carrageenans and their Derivatives.

PEMs are thin films formed by electrostatic interaction between oppositely charged polyelectrolytes. These are deposited alternately on a substrate using the layer-by-layer technique. We formed PEMs using chitosan as the polycation and carrageenan (and their derivatives) as the polyanion. Carrageenans and chitosan were each dissolved at 1 mg/mL in acetate buffer (pH 5.0) and stirred overnight at room temperature. Before polyelectrolyte deposition, the glass cover slip substrate was marked with unreactive stickers and placed in a 24-well plate. The unmarked side, which would be coated, was positioned upwards. The marked substrate was oxidized in vacuum chamber before use. The layer-by-layer deposition began with chitosan as the first layer, followed by carrageenan. For each layer, 0.3 mL of polyelectrolyte solution was added to the substrate in

the 24-well plate. The plate was then gently shaken for 5 minutes to allow for electrostatic interaction and adsorption. After each deposition, the polyelectrolyte was aspirated from the substrate and rinsed with 0.3 mL of pH 3.6 acetic acid for 4 minutes, with gentle shaking, to remove loosely bound polyelectrolyte. This process was repeated in alternating manner—chitosan followed by carrageenan—for a total of 16 layers, always ending with the modified carrageenan as the terminating layer.

3.2 Degradation Studies

Degradation of the modified carrageenan in solution and on PEM surfaces with lysozyme was carried out (Almodóvar et al., 2011). For degradation in solution, carrageenans and their carboxymethylated and aminated derivatives in solution in phosphate-buffered saline (PBS) buffer (pH 7.4) at 1 mg/mL were mixed with an equal volume of lysozyme solution at 0.01 mg/mL. Chitosan (1 mg/ml) in acetate buffer (pH 5.0) was also equally mixed with lysozyme solution (0.01 mg/ml) as positive control. The mixtures were incubated for 10 days at 37 °C. At 0, 3, 7, and 10-day intervals. The amount of reducing sugar ends were analyzed using the *p*-hydroxybenzoic acid hydrazide (pHBH) assay. For aminated lambda carrageenan, ALC, which is soluble at basic pH of 8.5 and above, its solution and lysozyme solution were prepared using borate buffer. For the standard solution, glucose solution was incubated in lysozyme solution in a 1:1 ratio at the same time interval used for carrageenan samples and partial inhibition of the assay was observed for lysozyme concentrations above 0.01 mg/ml. This degradation procedure was also applied to chitosan acting as positive control in acetic buffer (pH 5.0)

For surface degradation studies, four replicates of each 16-layer polyelectrolyte multilayer (PEM) film assembled with modified carrageenans were incubated in 0.25 mg/mL lysozyme solution in PBS at 37 °C for 0, 3, 7, 14, and 21 days in a 24-well plate. The lysozyme solution was refreshed

weekly to maintain enzymatic activity. At each time point, samples were removed and washed three times with PBS and deionized water. Samples were analyzed using atomic force microscopy (AFM) in PBS (7.4). A V-shaped silicon nitride cantilever with a reflective gold-coated back, spring constant of 0.35 Nm-1, and a nominal radius of 20 nm was used in ScanAsyst mode. The peak force setpoint was set close to 2 nN using Bruker Nanoscope software. Topographical imaging and roughness were measured in three non-overlapping 5 μm x 5 μm areas at room temperature.

Control samples were incubated in PBS only and treated the same at each degradation time point to account for changes in the surfaces that are not caused by the enzyme.

3.2.1 pHBH Assay

At each time point used for degradation in solution, aliquots of the degradation mixture were carefully collected. Each aliquot was then diluted 1:1 with PBS to standardize the sample concentration. In a 96-well microplate, 50 μL of each diluted sample was pipetted into four replicate wells. Next, 150 μL of freshly prepared detection solution was added to each well, ensuring a 1:3 ratio of sample to reagent. The plate was incubated at 65 °C for 15 minutes before measuring absorbance at 410 nm using a microplate reader.

The detection solution was prepared by mixing equal volumes of 2% (w/v) *p*-hydroxybenzoic acid hydrazide (pHBH) in 0.5 M HCl and 2 M NaOH. D-Glucose (1 mg/mL in PBS) served as the standard and was serially diluted, while PBS alone was used as the blank. PBS plus detection solution (50:150 μL) was the negative control, and lysozyme solution (0.01 mg/mL) plus detection solution (50:150 μL) was used to check for background signal from lysozyme

3.3 Antioxidant Activity of Carrageenan and its Derivatives

The antioxidant activity of carrageenans and their carboxymethylated and aminated derivatives were assessed using 2,2-diphenyl-1-picrylhydrazyl (DPPH) assay, 2,2'-azino-bis (3-ethylbenzothiazoline-6-sulfonic acid), ABTS assay and ferric reducing antioxidant power (FRAP) assay.

3.3.1 DPPH Assay

The DPPH assay was employed to assess the ability of carrageenans and their derivatives to scavenge free radicals. This assay measures the ability of antioxidants to donate a hydrogen atom to DPPH• radical. Specifically, the assay detects the reduction of the stable DPPH• (2,2-diphenyl-1-picrylhydrazyl) radical to its non-radical form (DPPH-H) when it reacts with a hydrogen- or electron-donating antioxidant, thereby providing a quantitative measure of antioxidant activity.

The DPPH solution (0.5 mM in methanol) was mixed with carrageenan solutions (2000 to 31.25 μg/ml) in a 1:2 ratio. Specifically, 100 μL of polymer solution was mixed with 50 μL of DPPH in a 96-well plate, then incubated in the dark for 30 minutes. DPPH absorbs at 517 nm and reduced absorbance, measured with a microplate reader, indicates better antioxidant activity. For this assay, ascorbic acid (200 to 3.125 μg/ml) was used as the standard, while the DPPH solution plus PBS was used as a negative control. For the blank, PBS was mixed with methanol in a 2:1 ratio.

3.3.2 ABTS Assay

The ABTS assay measures the ability of antioxidants to quench (neutralize) the $ABTS^{+}$• radical cation through electron transfer (ET) or hydrogen atom transfer (HAT) mechanisms. (Dudonné et al., 2009). Briefly, the detection solution was prepared by mixing 0.387 mg/ml ABTS solution with 3.81 mg/ml potassium persulfate solution in a 56.7:1 ratio in the dark at room temperature for 16 hours. In a 96-well plate, serially diluted polymer solutions (2000 to 31.25 μg/ml) were mixed

with the detection solution in equal volume. After gentle shaking for 30 minutes, the absorbance was measured at 734 nm. Equal volume of detection solution and 6 Trolox (50 μg/mL) were used as the standard. For the negative control, 100 μL of the detection solution was mixed with 100 μL of water, and DI water was used as blank.

The radical scavenging activity of the sample for both DPPH and ABTS assay was calculated using the following eq. 1:

$$\text{RSA (\%)} = \frac{Abs.\ of\ control - Abs.\ of\ sample}{Abs.\ of\ control} \times 100 \quad (1)$$

3.3.3 FRAP Assay

For the FRAP assay, the detection solution was made by mixing 300 mM acetate buffer (pH 3.6), 10 mM TPTZ in 40 mM HCl, and 20 mM FeCl3·6H2O in a 10:1:1 ratio. In a 96-well plate, the carrageenans and their derivative solutions were serially diluted from 2000 to 31.25 μg/mL (1:1 dilutions) and were mixed with equal volume of the ferric detection solution at for 30 minutes. Readings were taking at 593 nm with Trolox solution at 50 μg/mL as standard, and a 1:1 mixture of the detection solution and DI water as negative control while DI water was used as the blank.

3.4 Antibacterial Activity of Carrageenan

Bacteria are classified as Gram-positive or Gram-negative based on structural differences in their cell walls, as revealed by the Gram staining technique (Kim et al., 2015). Gram-positive bacteria, including *Staphylococcus aureus*, have a thick peptidoglycan layer that provides rigidity but lacks an outer membrane, making them more susceptible to cell wall-targeting antibiotics and antimicrobial agents. Gram-negative bacteria, such as *Pseudomonas aeruginosa*, have a thin peptidoglycan layer placed across an outer membrane rich in lipopolysaccharides (Tavares et al., 2020). This outer layer serves as a strong barrier against many antimicrobial agents, making Gram-negative bacteria more resistant to antibiotics and posing a greater challenge in clinical infections.

In this experiment, *Staphylococcus aureus* and *Pseudomonas aeruginosa* were used for evaluating the antibacterial ability of carrageenan and its derivatives (Chae et al., 2020b; Madruga et al., 2020). The strains were maintained either on nutrient agar (HIMEDIA®, India) at 4 °C or preserved in beads at −80 °C.

The antibacterial activity of carrageenans and their derivatives were assessed using the broth microdilution method in Mueller–Hinton Broth (MHB), following Clinical and Laboratory Standards Institute (CLSI) guidelines. Briefly, 100 µL of bacterial suspension (1×10^6 CFU mL^{-1}) was combined with 100 µL of polymer solution at concentrations ranging from 0.063 to 1.0 µg $µL^{-1}$ in 96-well plates. The plates were incubated at 37 °C for 2, 4, 6, 8, 10, 18 and 24 h. Sterile broth without bacteria was used as the negative control, while cultures without polymer served as the positive growth control.

After incubation, bacterial growth was determined by measuring optical density at 595 nm using a microplate reader and the most optimum condition for bacterial growth inhibition was selected for discussion.

3.4.1 Analytical Characterization of Modified Carrageenan

Modified samples were dissolved in D_2O at a concentration of 10 mg/ml overnight, and ^1H and ^{13}C NMR were performed using a method similar to that described previously (Madruga et al., 2020). For the ^1H NMR, 65 scans were taken at a pulse angle of 90° at 338 K. Additionally, an acquisition time of 4.2 seconds and an interpulse delay of 5.0 seconds were used on a Bruker NEO US 400 NMR spectrometer operating at 400 MHz. A total of 10,000 scans were used for the ^{13}C NMR at a pulse angle of 90°, with an acquisition time and interpulse delay of 1.2 s and 1.0 s, respectively. Also, Fourier-Transform Infrared Spectroscopy (FTIR) spectra of unmodified,

carboxymethylated and aminated carrageenan were obtained using an ATR-FTIR microscope (PerkinElmer Spotlight 400) over the range 4000–400 cm^{-1}.

3.4.2 Degree of Substitution (DS) for Carboxymethylation

The degree of substitution for the hydroxyl group by carboxymethyl was evaluated using a similar method described in literature (Madruga et al., 2020). The ^{1}H NMR spectra of each carrageenan and its derivative were overlaid for comparison using the MNOVA software. To calculate the average degree of substitution, the peaks associated with the methylene protons (from 3.4 ppm to 5.2 ppm) were integrated to get its area and then calculated using the formula in Eq. 2 and 3.

$$DS = \sum x_i \quad (2)$$

$$x_i = \frac{A\,[proton(s)\ of\ Carboxylmethylat \quad carrageenan\ at\ O_i]}{A\,[proton(s)\ of\ native\ carrageenan\ at\ O_i] + A\,[proton(s)\ of\ Carboxylmethylated\ carrageenan\ at\ O_i]} \quad (3)$$

Where O_i is the oxygen atom at position i (site of substitution on the carrageenan disaccharide unit) and A represents the peak area.

3.5 Degree of Substitution for Amination

The degree of amination was calculated after quantifying the amine content using the 2,4,6-trinitrobenzenesulfonic acid (TNBS) assay (Malyarenko et al., 2020). Briefly, for the TNBS assay, the aminated samples were dissolved overnight in 0.1 M sodium tetraborate decahydrate buffer (pH 8.5) at a concentration of 1 mg/mL, then serially diluted in a 1:1 ratio using the buffer to obtain solutions of the sample with lower concentrations. These different dilutions of the sample were mixed with an equal volume of TNBS solution (0.2 mg/mL) in 96-well plates and incubated for 2 hours at 37 °C. Using a microplate reader, the absorbance at 405 nm was measured. Glucosamine at 1 mg/ml and its 1:1 serial dilutions were used as the standard to get glucosamine equivalent for the aminated carrageenan. This equivalent is substituted into the eq. 4 below to calculate the DS.

$$DS = \frac{Eq_{mg/ml} \cdot MW_{repeat\ unit}}{MW_{glucosamine} \cdot\ m_{polymer} \cdot 1000} \quad (4)$$

$Eq_{mg/ml}$ represents amine equivalent from the TNBS calibration. $MW_{glucosamine}$ and $MW_{repeat\ unit}$ represent the molecular weights of glucosamine and one repeating disaccharide unit of carrageenan respectively. $m_{polymer}$ is the polymer concentration in mg/ml and 1000 is the conversion factor from mg to g.

3.6 Statistical Analysis

It was ensured that for the various experiments like the antibacterial evaluation, chemical modification, degradation studies and antioxidants activity, no less than 3 replicates were used ($n \geq 3$) and the results are all reported as mean ± standard deviation. One-way Analysis of Variance (ANOVA) was performed to assess the statistical differences between groups followed by Tukey's honest significant difference test as a post-hoc analysis with a confidence level of $p < 0.05$.

4. Results and Discussion

4.1 Characterization of Carboxymethylated and Aminated Carrageenan

4.1.1 ^{1}H and ^{13}C NMR Spectra and Degree of Substitution (Ds) of Carboxymethyl Carrageenan

The ^{1}H and ^{13}C NMR spectra for the kappa-, iota-, and lambda-carrageenans and their derivatives are shown in the figures below. For kappa- and iota-carrageenan, and their derivatives, their spectra are similar to those already published (Aparna et al., 2018; Jumaah et al., 2015; Madruga et al., 2020). Both ^{1}H spectra of KC and CMKC in fig. 1 show peaks in the range of 3.7 to 5.6 ppm indicating that the structure of these polysaccharides remained intact after the reaction. The new peaks at 3.89 ppm, 4.17 ppm, and 4.38 ppm observed for CMKC correspond to the methylene protons of the carboxymethyl group substituting for the OH group at the C-2 of DA (3,6-anhydro-α-D-galactopyranose) unit and C-2 and C-6 of the G (β-D-galactopyranose) units. The success of this modification was supported by ^{13}C NMR in fig. 2, which showed new peaks at 177.74 ppm, 177.53 ppm, and 121.07 ppm, not present in the native or unmodified kappa carrageenan, corresponding to the carbon of the C=O group and the C-C group introduced.

A similar result was observed for modified iota carrageenan shown in fig. 3, matching what has been previously published (Jumaah et al., 2015). Fig. 3 shows new peaks at 3.94 ppm and 4.18 pm indicate methylene protons from the new functional group at position C-2 and C-6 of the β-D-galactopyranose-4 sulfate unit. These are not present in the original iota carrageenan and confirm successful substitution of the OH-group.

The ^{1}H NMR spectra of the LC and CMLC is shown in fig. 4. The CMLC spectrum shows new peaks at chemical shift of 3.92 ppm and 4.4 ppm corresponding to the methylene protons in the carboxymethyl group at position C-4 and C-6 of the G unit, which are absent in the LC spectrum.

Additionally, the ^{13}C spectra of LC and CMLC (fig. 5) showed a new peak at a chemical shift of 177.36 ppm, corresponding to the carbonyl of the carboxylate group, attributed to the position of the carboxymethyl group on the CMLC. This evidence supports the success of the modification.

The degree of substitution (DS), defined as the number of carboxymethyl groups per disaccharide unit, was determined for CMKC, CMIC, and CMLC using their respective ^{1}H NMR spectra and Equation 3. The calculated DS values were 1.26 for CMKC, 0.94 for CMIC, and 0.86 for CMLC, as summarized in Table 1.

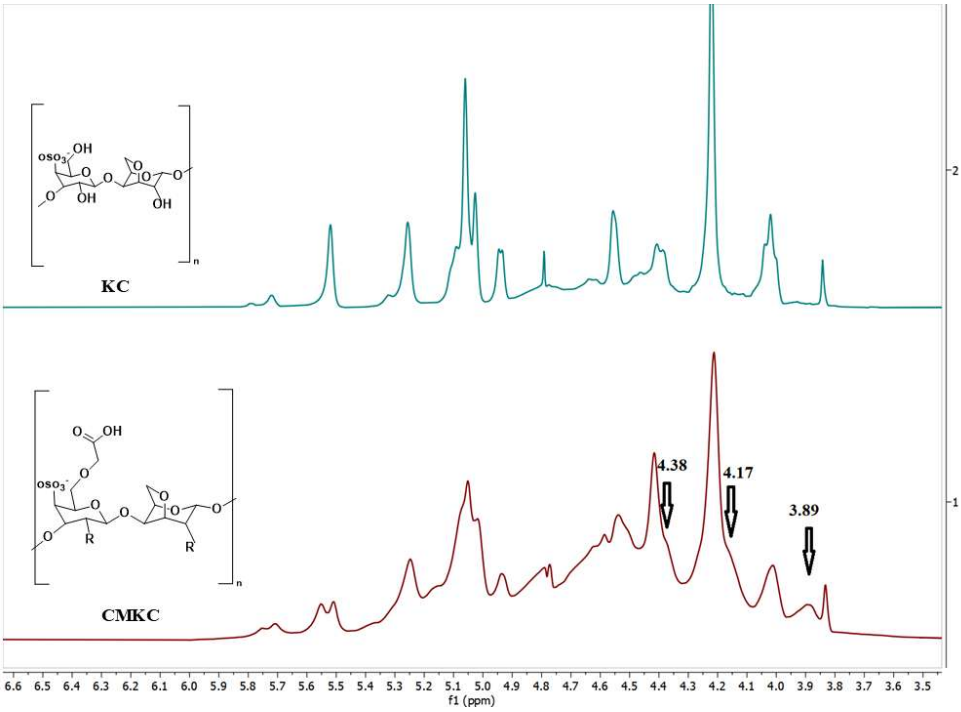

Figure 1: ^{1}H NMR spectra of KC and CMKC from Williamson ether synthesis.

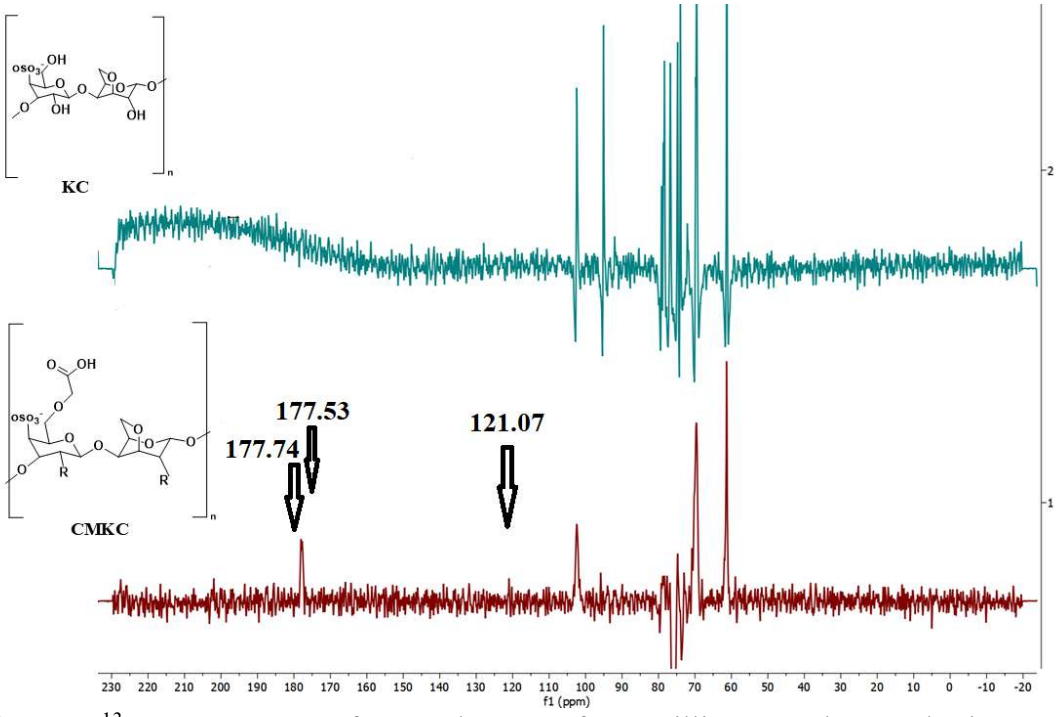

Figure 2: ^{13}C NMR spectra of KC and CMKC from Williamson ether synthesis.

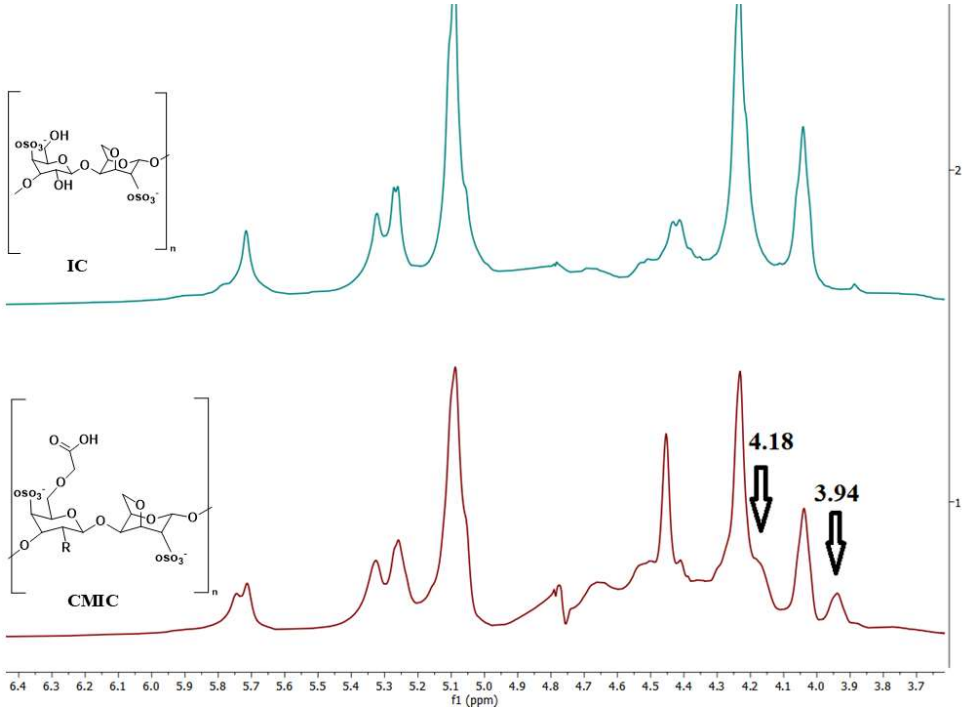

Figure 3: ^{1}H NMR spectra of IC and CMIC from Williamson ether synthesis.

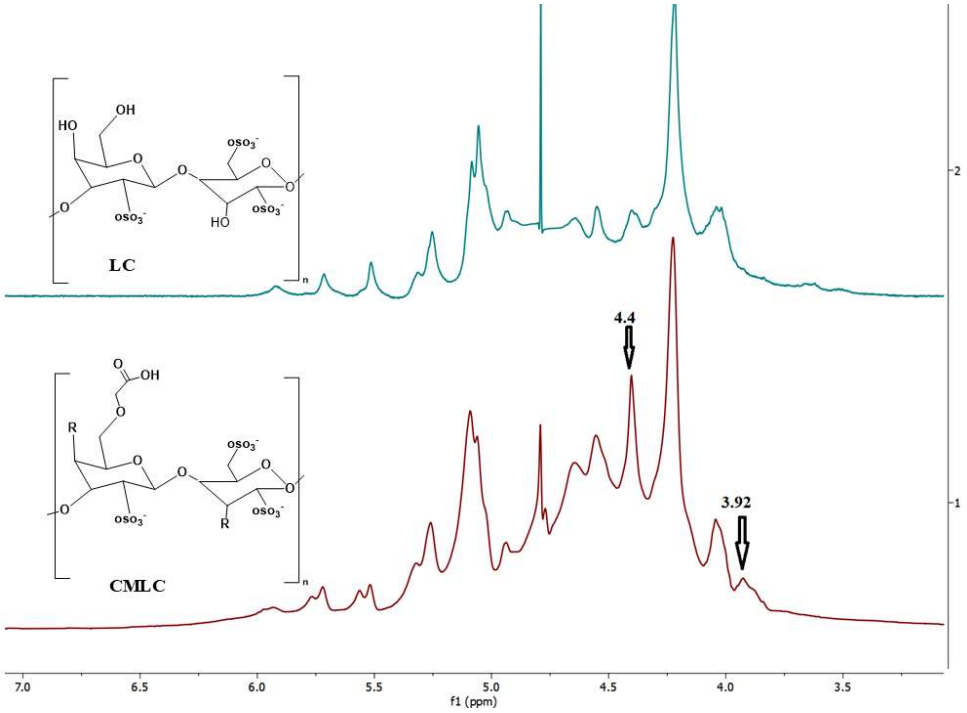

Figure 4: ^{1}H NMR spectra of LC and CMLC from Williamson ether synthesis.

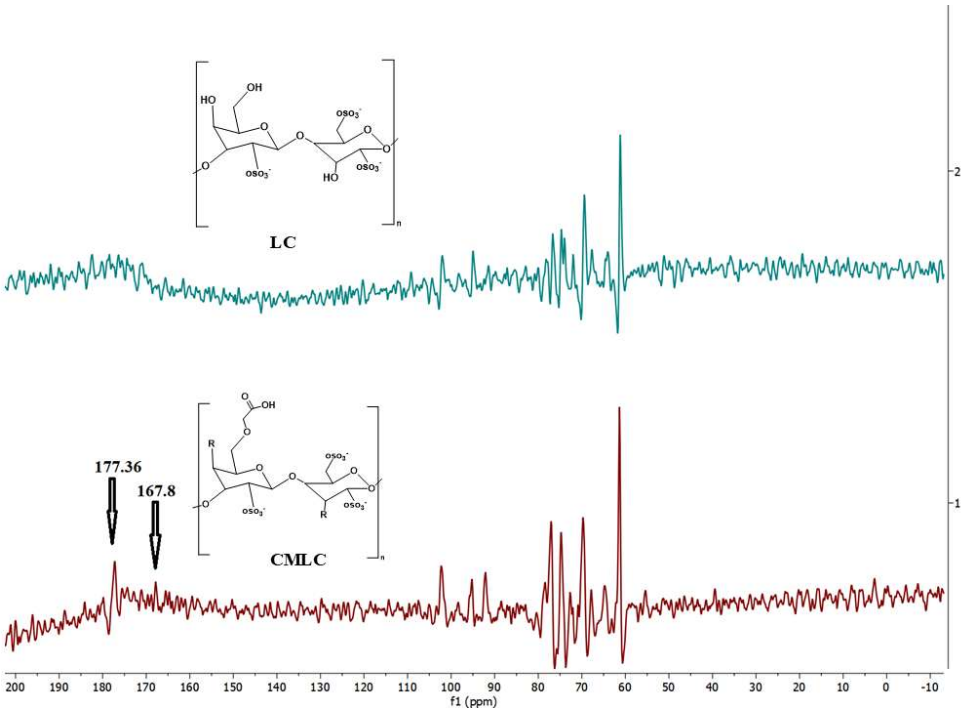

Figure 5: ^{13}C NMR spectra of LC and CMLC from Williamson ether synthesis.

4.1.2 ^{1}H and ^{13}C NMR Spectra and Degree of Substitution (DS) of Aminated Carrageenan

Among the different reaction routes employed for the amination of carrageenan, the epichlorohydrin and ammonium hydroxide chemistry was the most successful and reproducible. Fig. 6 shows the spectrum of the product obtained from the KC possible amination, using the nucleophilic substitution method. ^{1}H NMR showed a weak signal representing a new proton peak at δ 3.63 ppm, attributed to the –CH_2– group adjacent to the introduced amine, suggesting minimal substitution. However, with the TNBS assay, this amine content was below the detection limit and could not be quantified. These indicate no possible incorporation of the amine group by this chemistry likely due to low reactivity at the basic conditions used.

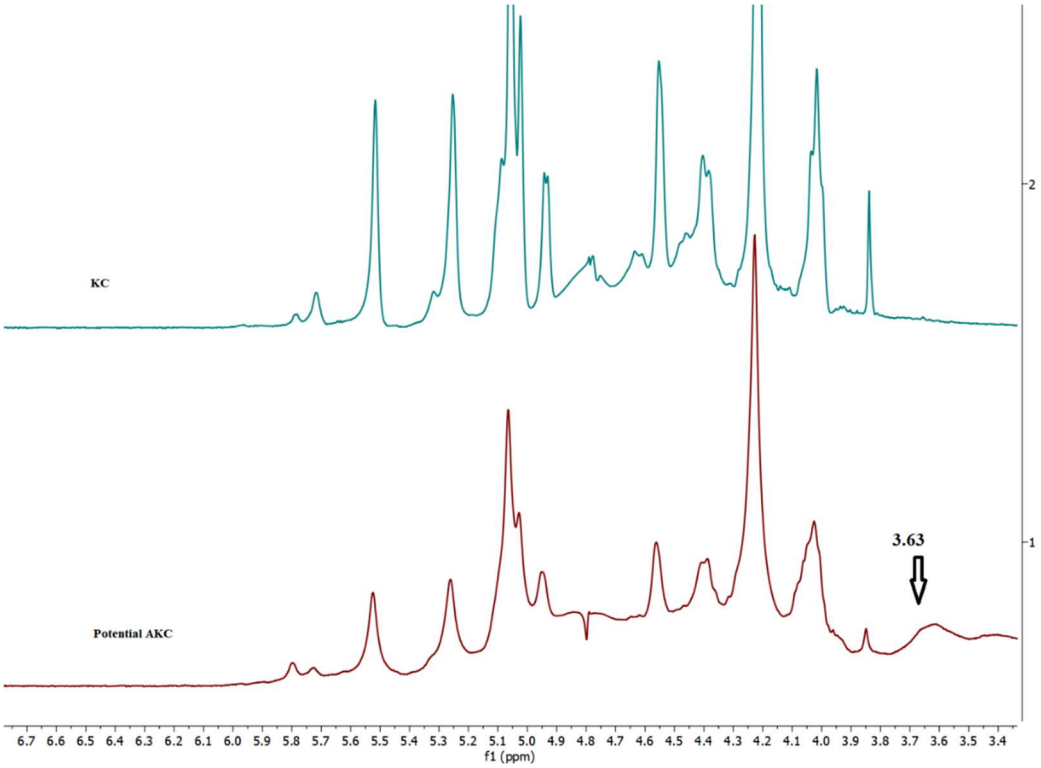

Figure 6: ^{1}H NMR spectra of KC and potential AKC from nucleophilic substitution synthesis.

Due to the ineffectiveness of the nucleophilic substitution method, we attempted to aminate the carboxymethylated carrageenans employing two carbodiimide coupling agents that can form amides between carboxylic acids and amines (EDC and DMTMM), using ethylene diamine. The

carboxyl group in CMKC forms an unstable *O*-acylisourea intermediate with EDC which could be stabilized by *N*-hydroxysuccinimide (NHS). Fig. 7, shows ^{1}H NMR of the possible aminated product with new peaks at 3.77 ppm with very high intensity and 3.63 ppm, corresponding to methylene protons next to the free amine ($–CH_2–NH_2$) and amide bond ($–CH_2–NH–CO–$). Other peaks at 2.42, 2.31, 1.58, and 1.47 ppm, suggested the presence of EDC-related byproducts. More evidence from ^{13}C NMR in fig. 8 showed three additional peaks at 39.8, 38.6 and 36.4 ppm likely from the EDC coupling aside the from the possible amine peaks at ~43.3 ppm typical of carbon bonded to nitrogen. With TNBS assay, the DS of the product of this reaction was calculated to be 4.89 for CMKC which is theoretical above the maximum DS of 3. After dialysis against $MgCl_2$, the DS drops to 0 in the TNBS assay. This phenomenon also suggested that the amine groups were from ionically associated ethylenediamine and possibly from an EDC intermediate, and not from covalently attached ethylenediamine.

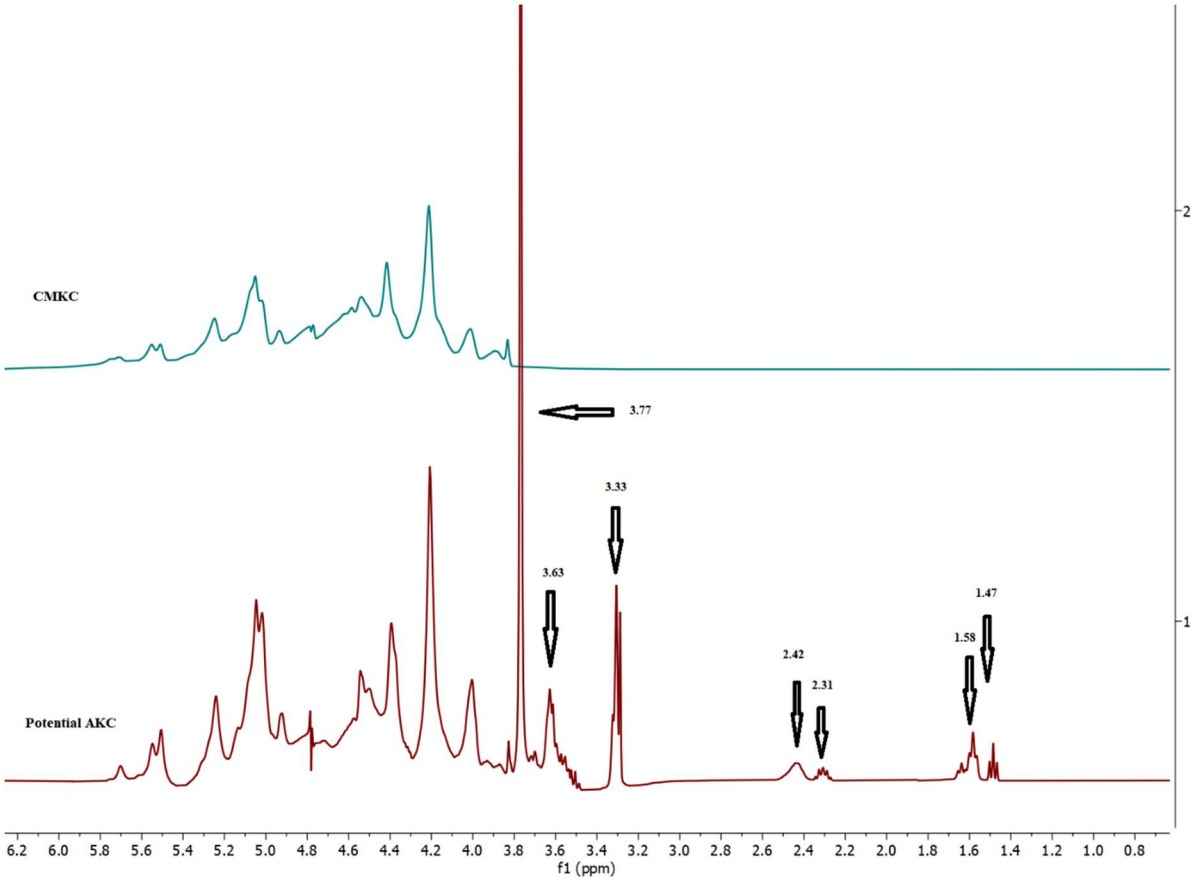

Figure 7: ^{1}H NMR spectra of KC and potential AKC from EDC coupling.

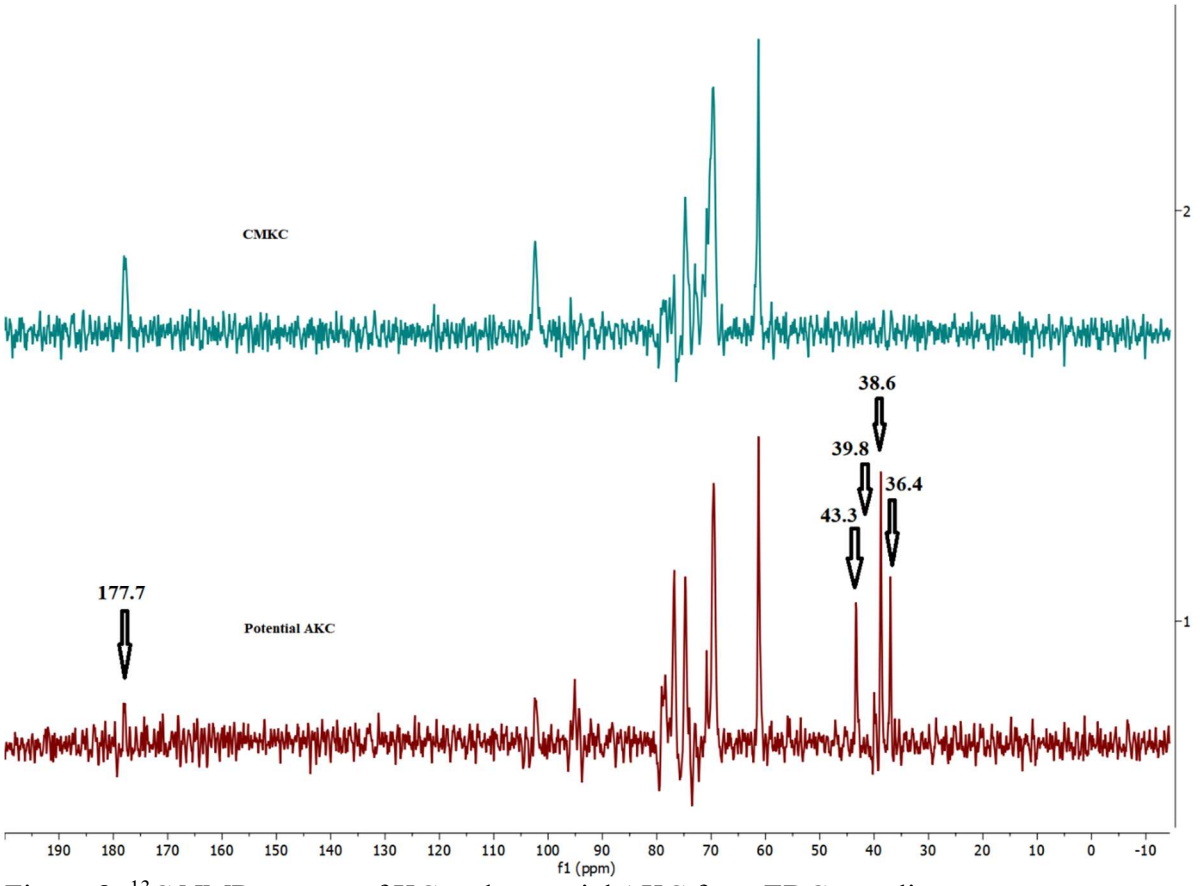

Figure 8: ^{13}C NMR spectra of KC and potential AKC from EDC coupling.

Similar observations were made with DMTMM coupling. ^{1}H NMR of the CMKC+DMTMM intermediate (fig. 9) revealed new peak with a very high intensity at 3.54 ppm and multiplet peaks between 4.14–4.30 ppm, possibly reflecting the presence of triazine and morpholinium fragments from DMTMM conjugation. After EDA addition, the final product displayed new peaks at 3.65 ppm and 3.77 ppm typical of carbon bonded to nitrogen as seen in fig. 9. This result is similar to that observed with the EDC, however the spectrum of the DMTMM looked cleaner, indicative of less DMTMM byproduct in the final sample. Also, the ^{13}C NMR of the final product of this reaction in fig. 10 shows a new signal at 37.3 ppm, which may correspond to methylene carbons near nitrogen, but with higher intensity than expected. The 91.83 ppm peak was unusually upfield and may have come from unreacted DMTMM or triazine structures. The DS for this product

calculated using the TNBS assay was 4.5, indicating over-amination. After dialysis against $MgCl_2$ the TNBS result dropped below the detectable limit of amine, indicating that this method resulted in only ionically, not covalently associated ethylene diamine.

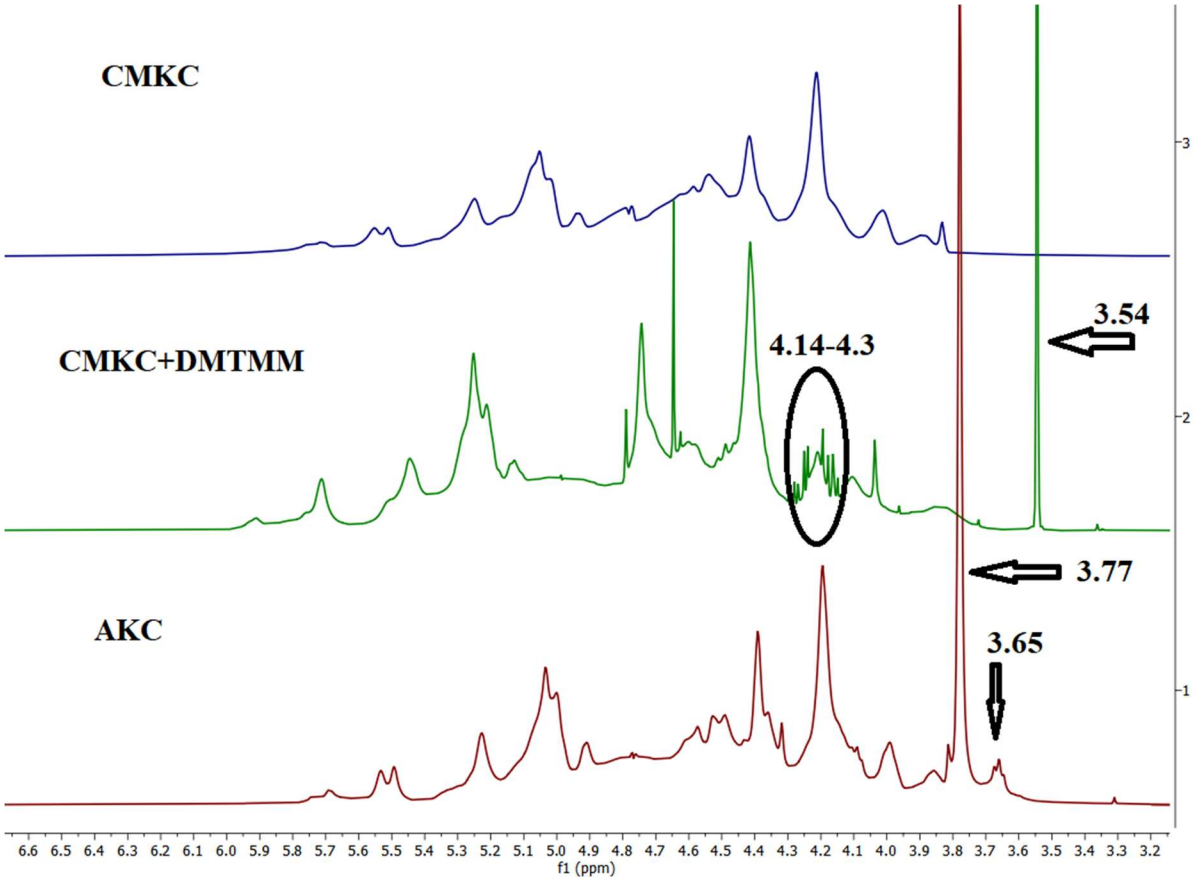

Figure 9: ^1H NMR spectra of KC, the KC-DMTMM intermediate, and potential AKC from DMTMM coupling.

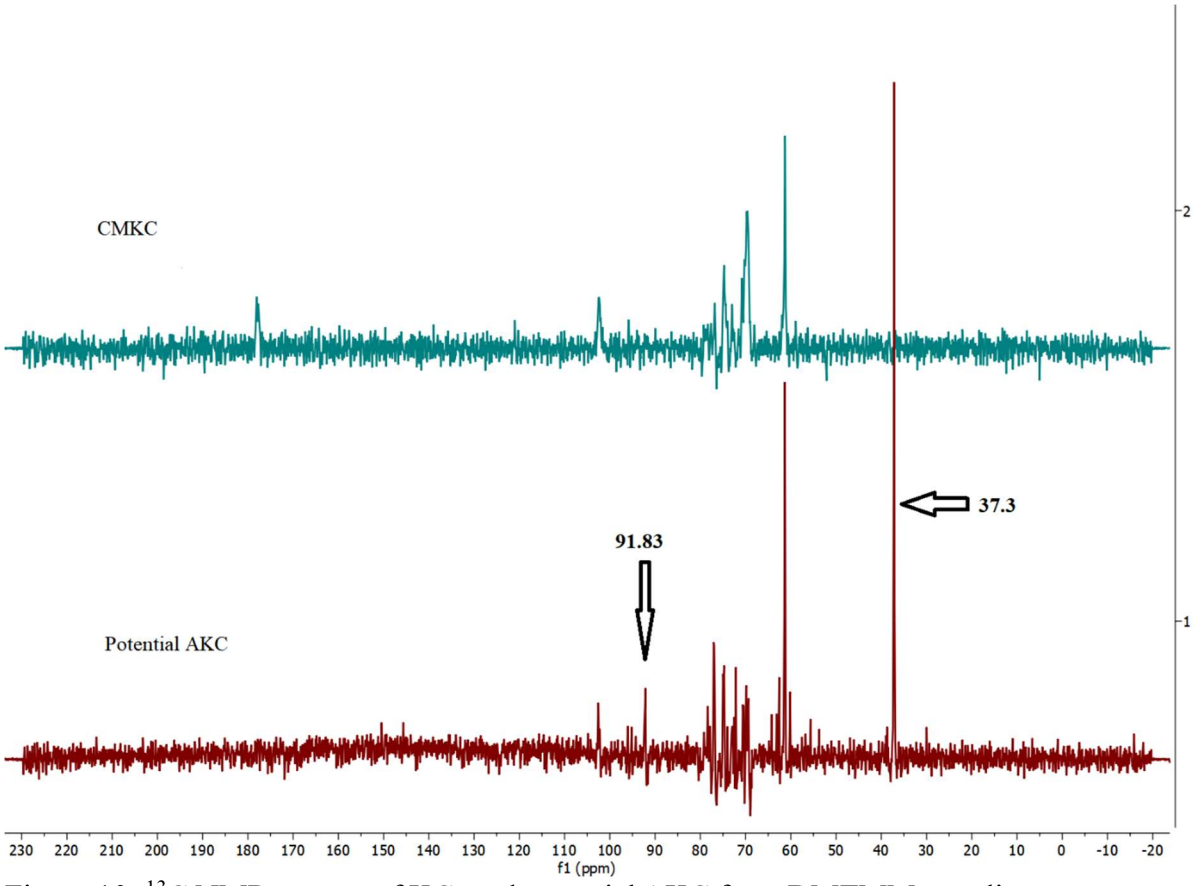

Figure 10: ^{13}C NMR spectra of KC, and potential AKC from DMTMM coupling.

The last and successful chemistry employed was epichlorohydrin-ammonium hydroxide chemistry. This reaction replaces the OH group on the polysaccharide backbone with a primary amine tethered through a 2-hydroxy-3-aminopropylether ether linkage (-O-CH_2-CH(OH)-CH_2-NH_2). The success of this modification was confirmed by ^1H, ^{13}C NMR, and amine content measurement, to form AKC and ALC from the amination of native KC and LC respectively using this chemistry. The amination of IC results in an insoluble product.

Fig. 11 shows stacked ^1H NMR spectra of KC and derivative (AKC) with characteristic proton signals for the polysaccharide backbone (3.3–5.4 ppm) remaining intact for both spectra. The ^1H NMR of the AKC spectrum in fig. 11a shows a multiplet peak centered at 3.32 ppm, attributed to methylene protons adjacent to the introduced amine groups. The corresponding ^{13}C NMR spectra

in fig. 12 shows three new, well-defined peaks at 42.8 ppm, 43.3 ppm, and 67.07 ppm, corresponding to CH_2–NH_2, CH_2–O–carrageenan, and CH–OH groups, respectively. These peaks confirmed the successful incorporation of the amine group to the native kappa carrageenan with DS of 1.12 after $MgCl_2$ dialysis.

A similar reaction was carried out with iota-carrageenan, but the resulting product was insoluble across a wide pH range. This insolubility likely resulted from crosslinking of carrageenan chains during the initial reaction step in the presence of NaOH and epichlorohydrin, as evidenced by gel formation. Such crosslinking reduces the availability of epoxide groups for nucleophilic attack by the amine groups of ethylenediamine (EDA), thereby hindering the intended amination reaction.

Fig. 13 shows the ^{1}H NMR of aminated LC (ALC) compared to native LC. In the ALC spectrum, new single signal at 3.1 ppm and multiplet signals at 3.56-3.39 ppm were present. These peaks correspond to the methylene group adjacent to the amine and the adjacent CH-OH group. The broad multiplet at 3.56-3.39 ppm results from nonequivalent diastereotopic methylene protons coupled to the neighboring hydroxyl-bearing carbon. Also, in fig. 14, the ^{13}C NMR further confirms the modification. New peaks at 51.5 and 42.83 ppm are assigned to the CH_2–NH_2 and CH(OH) carbons of the hydroxypropyl chain. The TNBS assay gave an amine content of 3.9 umol NH_2/mg lambda carrageenan with a DS of 1.3 after $MgCl_2$ dialysis.

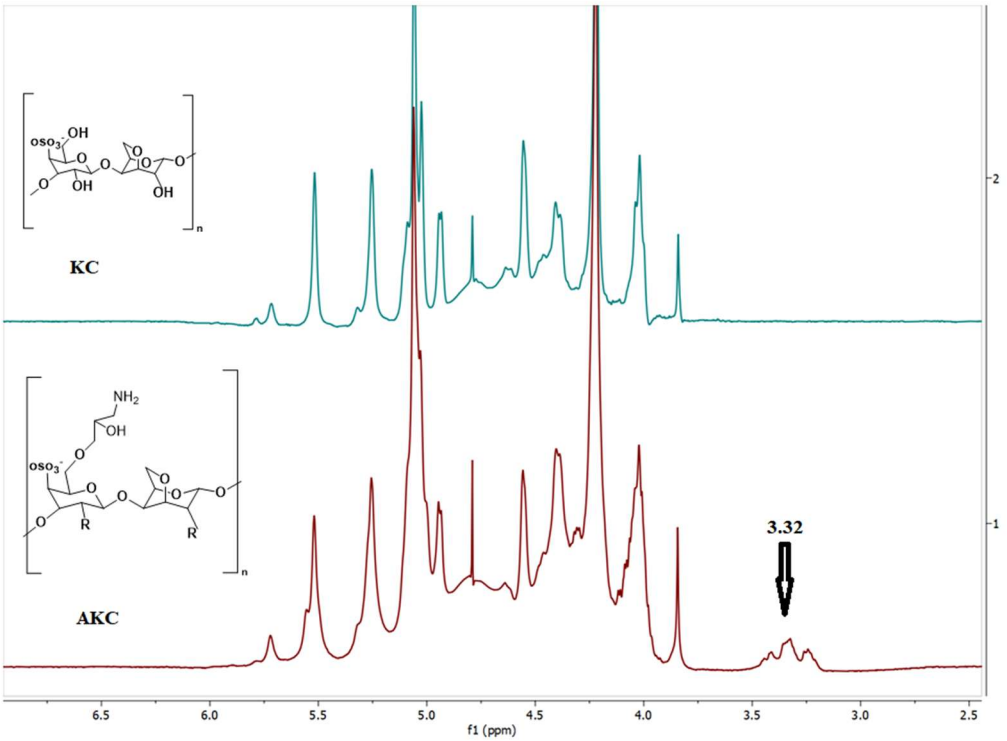

Figure 11: ^{1}H NMR spectra of KC and AKC from epichlorohydrin-ammonium hydroxide chemistry.

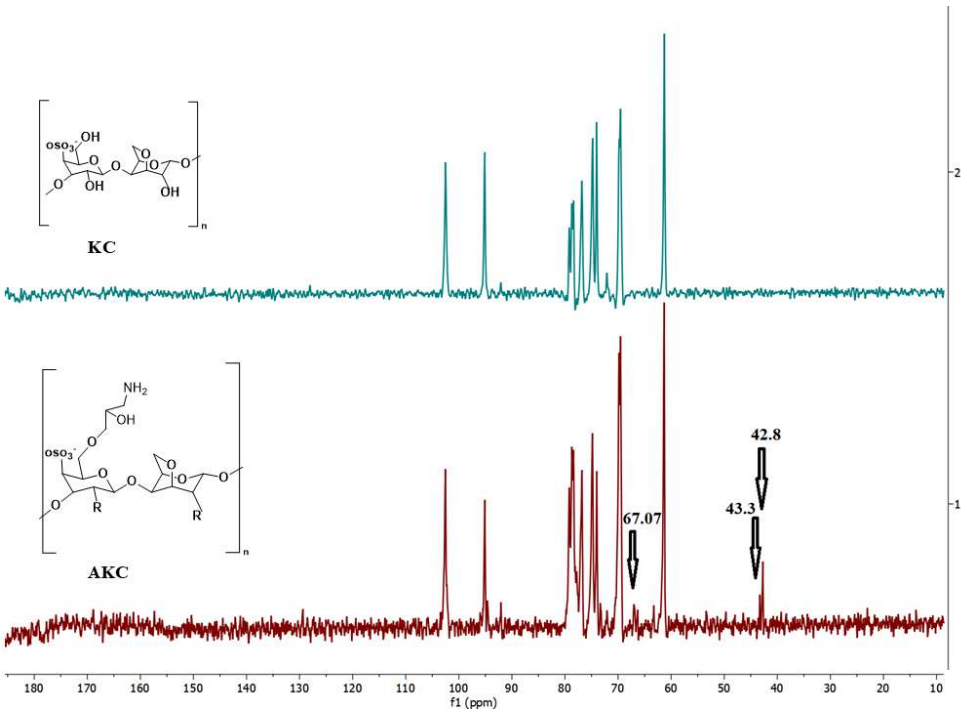

Figure 12: ^{13}C NMR spectra of KC and AKC from epichlorohydrin-ammonium hydroxide chemistry.

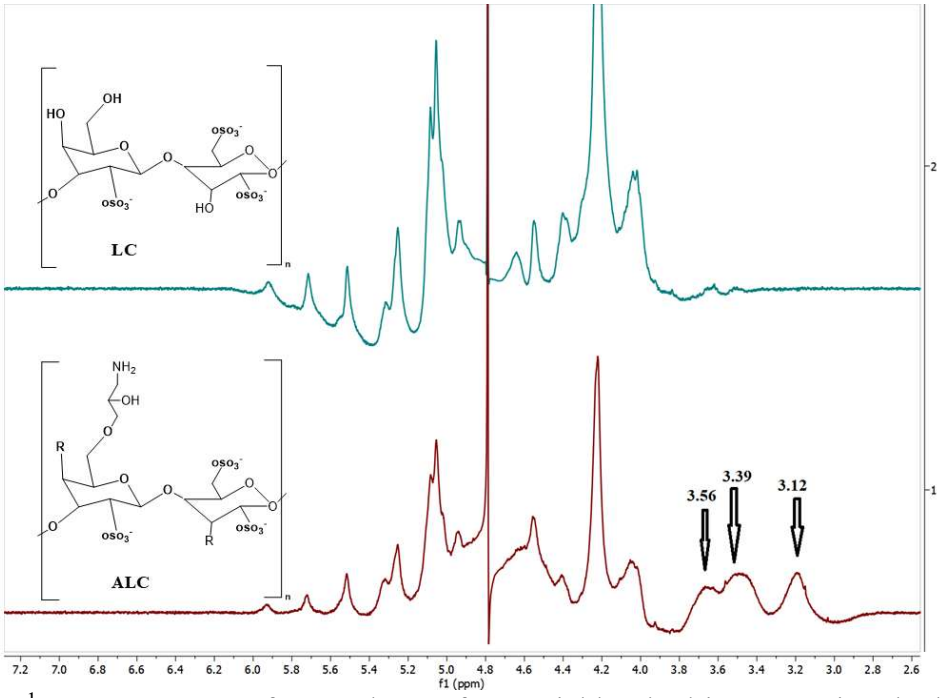

Figure 13: ^{1}H NMR spectra of LC and ALC from epichlorohydrin-ammonium hydroxide chemistry.

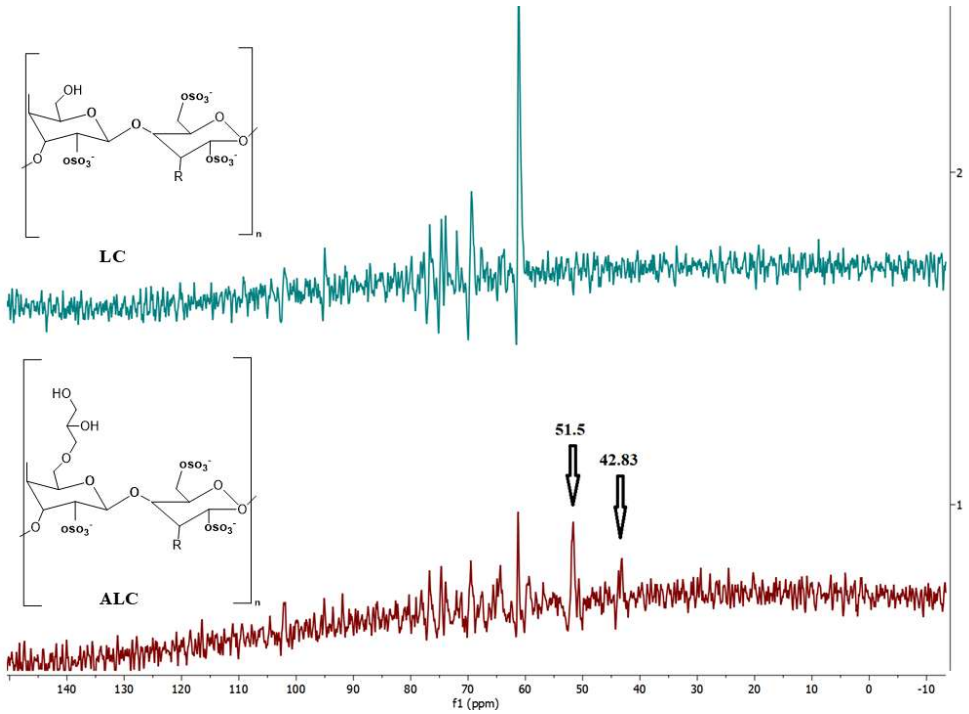

Figure 14: ^{13}C NMR spectra of LC and ALC from epichlorohydrin-ammonium hydroxide chemistry.

Table 1: Degree of substitution (DS) values for carboxymethylated and aminated carrageenan derivatives.

Carrageenan derivatives	DS
CMKC	1.26
CMIC	0.94
CMLC	0.86
AKC	1.12
ALC	1.3

4.1.3 Fourier-Transform Infrared Spectroscopy (FTIR) Of Carrageenans and their Derivatives

Functional groups resulting from the carboxymethylation reaction of kappa-, iota-, and lambda-carrageenans were also confirmed using FTIR as shown in fig. 15. For CMKC, the appearance of peaks at 1593 cm^{-1} and 1423 cm^{-1}, absent in KC, represent the asymmetric and symmetric stretching vibrations of carboxylate (-COO-) groups and confirms the presence of carboxymethyl group. KC shows a broad peak at 1630 cm^{-1}, likely due to bound water and residual O-H bending. Additionally, for the CMKC, the peak at 1330 cm^{-1}, which is absent in the KC, is associated with C-H bending of the methylene group, further confirming the success of the reaction. Both spectra of CMKC and KC display peaks around 1224-1225 cm^{-1}, 1030-1150 cm^{-1}, and 928-926 cm^{-1} for the S=O stretching vibration of the sulfate ester group, C-O and glycosidic ring-related bands, and C-O-C glycosidic bridge, respectively. These suggest that the main structure of the polysaccharide was preserved after the modification.

Also, in fig. 15, the FTIR results confirm the structure of carboxymethylated iota carrageenan (CMIC). New peaks at 1600 cm^{-1} and 1423 cm^{-1} correspond to asymmetric and symmetric stretching vibrations of carboxylate anions (-COO-). The peak at 1327 cm^{-1}, which is absent in the

IC, is associated with C-H bending of the methylene group. These are absent in the IC spectrum, confirming successful substitution of the hydroxyl group with the carboxymethyl group. Just as in CMKC, the main structure of CMIC when compared to IC remain intact after this modification. Figure 15 also shows a similar result for CMLC. New peaks at 1601 cm^{-1} and 1422 cm^{-1} appeared in CMLC and are attributed to the asymmetric and symmetric vibrations of the carboxylate groups (-COO-). These peaks are absent in LC, confirming carboxymethylation.

In fig. 16, AKC shows peak shift and increased intensity at 3388 cm^{-1} due to N-H bending vibrations of the amine group, which overlap the existing O-H bending region seen in KC at 3385 cm^{-1}. The shoulder peak at 2920 cm^{-1} likely indicates C-H stretching of methylene groups from the epichlorohydrin linker. A similar trend was observed for ALC, with peaks at 3388 cm^{-1}, which are broadened and slightly shifted bands attributed to the new N-H stretching vibrations overlapping with the existing O-H vibrations on the LC spectrum at 3413 cm^{-1}.

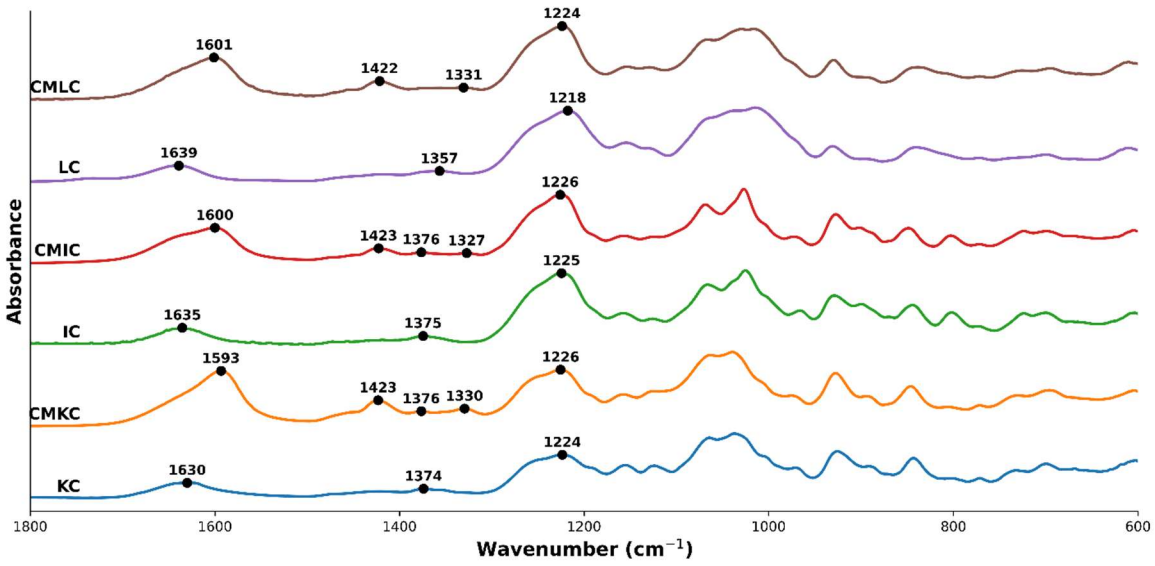

Figure 15: FTIR spectra of native and carboxymethyl carrageenans (KC, CMKC, IC, CMIC, LC, CMLC).

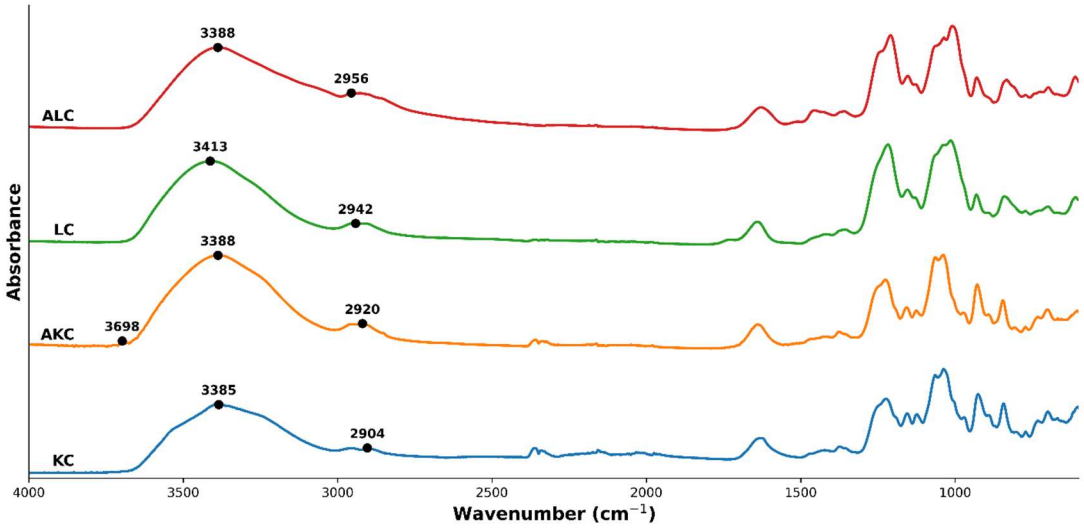

Figure 16: FTIR spectra of native and aminated carrageenans (KC, AKC, LC, ALC).

4.2 Antioxidant Activity of Carrageenans and their Derivatives

4.2.1 DPPH Radical Scavenging Activity (RSA)

The antioxidant potential of native and chemically modified carrageenan derivatives was evaluated using the DPPH (2,2-diphenyl-1-picrylhydrazyl) radical scavenging assay at a concentration of 1 mg/mL. The results, expressed as radical scavenging activity percentage (RSA%), are shown in fig. 17.

Among the three unmodified carrageenan, IC (iota carrageenan) exhibited the highest antioxidant activity (40.4 ± 3.5%), followed by LC (lambda carrageenan) at approximately 35%, and KC (κ-carrageenan) at the lowest with only 12.6 ± 2.8%.

Carboxymethylation generally improved RSA% in all backbones. For instance, CMKC showed a significant increase to 27.4 ± 5.5%, more than doubling the activity of the native KC. However, CMIC showed lower RSA% (25.0 ± 3.3%) than unmodified IC (40.3 ± 4.2%), possibly due to substitution at reactive sites interfering with sulfate-mediated activity. Interestingly, CMLC maintained RSA value slightly higher than LC, suggesting that carboxymethylation in LC did not significantly change its antioxidant behavior and may have offered stability.

In contrast, aminated derivatives (AKC and ALC) showed lower antioxidant performance, particularly AKC, which recorded the lowest RSA% (5.8 ± 7.0%) of all samples. This result aligns with the expectation that introduction of positively charged amine groups does not contribute to radical scavenging and may instead reduce the availability of hydroxyl or sulfate groups that typically donate electrons in antioxidant mechanisms.

Overall, at 1 mg/ml, the results suggest that carboxymethylation is effective in increasing antioxidant activity in carrageenan derivatives and supports the idea that carboxymethyl groups introduce electron-donating capacity and increase hydrophilicity, both of which are beneficial for free radical scavenging. While amination reduces the availability of active hydroxyl and sulfate sites responsible for electron transfer.

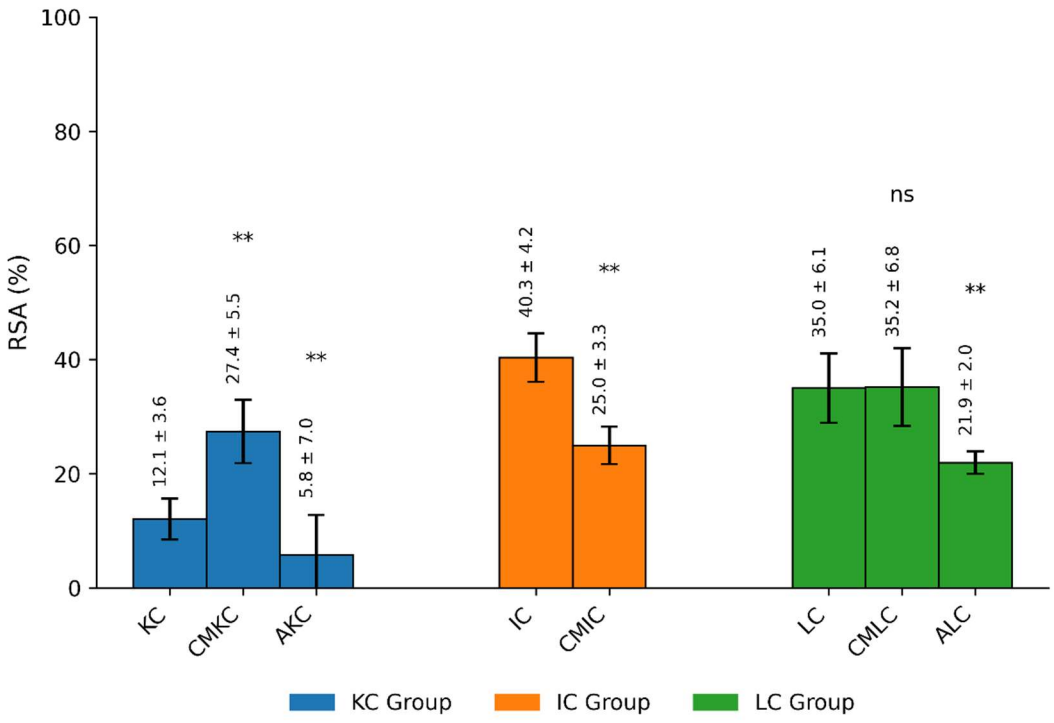

Figure 17: DPPH radical scavenging activity (RSA%) of native and modified carrageenans at 1 mg/mL.** indicates statistically significant difference relative to the corresponding unmodified carrageenan ($p < 0.01$).

4.2.2 ABTS Radical Scavenging Activity

In addition to DPPH, the ABTS assay was performed to evaluate the antioxidant activity of native and modified carrageenan derivatives at 1 mg/mL. The ABTS method is responsive to radical scavengers capable of quenching the $ABTS^{+}$• cation radical. The results are shown in fig. 18 and reported as RSA% (radical scavenging activity percentage).

In the KC group, CMKC improved ABTS activity from 7.3% to 12.4%, consistent with the idea that introducing carboxyl groups may increase solubility and possibly enhance interaction with the ABTS radical. However, for the IC group, CMIC had a reduced RSA% (6.9%) compared to native IC, which may reflect structural changes or reduced exposure of sulfate groups involved in radical interaction. CMLC, on the other hand, showed a moderate increase from 7.9% to 16.4%, indicating a possible benefit of carboxymethylation in the LC backbone.

In the LC group, ALC nearly quenched the ABTS radical, with an RSA value of 98.5%. This is far beyond the activity observed for any other sample in this study. Since it was dissolved in borate buffer (pH 8.5) for solubility, a control experiment with Trolox in borate buffer and in just borate buffer showed no antioxidant activity, indicating that the antioxidant activity was inherent after modification and not due to the buffer.

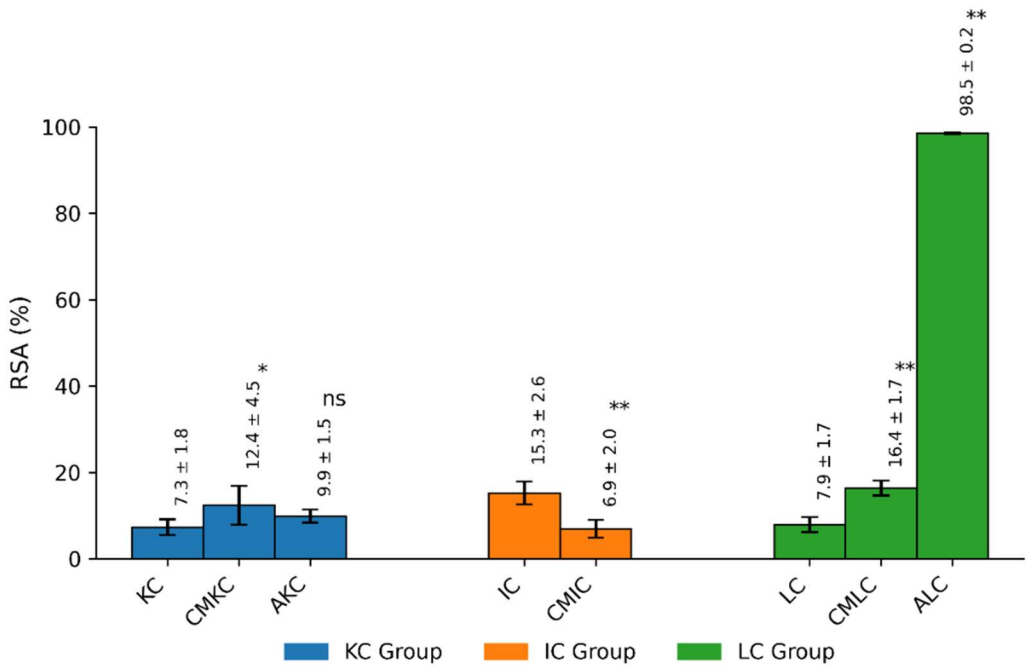

Figure 18: ABTS radical scavenging activity (RSA%) of native and modified carrageenans at 1 mg/mL. * indicates $p < 0.05$ and ** indicates $p < 0.01$, relative to the corresponding unmodified carrageenan.

4.2.3 Ferric Reducing Antioxidant Power (FRAP) Assay

The FRAP assay was used to measure the antioxidant activity of the carrageenan samples based on their ability to reduce ferric ions (Fe^{3+}) to ferrous ions (Fe^{2+}). The results are expressed in terms of Trolox equivalents (mg/mL), which reflect the reducing power of each sample compared to a Trolox standard. The assay was performed at a sample concentration of 1 mg/mL, and the results are shown in fig 19.

Interestingly, carboxymethylation did not improve FRAP values in most cases. Both CMKC and CMIC had values which were not significantly different from their native forms. This could mean that the addition of carboxyl groups does not significantly enhance the electron-donating ability of the polymer. However, CMLC showed a small improvement (2.45 mg/mL). Among the aminated derivatives, AKC displayed no significant difference from KC. In contrast, ALC showed a

noticeable improvement. This indicates that the presence of sulfate groups may enhance the polymer's ability to reduce ferric (Fe^{3+}) to ferrous (Fe^{2+}) ions. However, due to the difference in pH, it is likely that the activity of AKC in the elevated pH of 8.5 could differ from its activity in PBS (7.4). Trolox control was done in PBS (7.4) for AKC and CMKC and in borate buffer (8.5) for ALC.

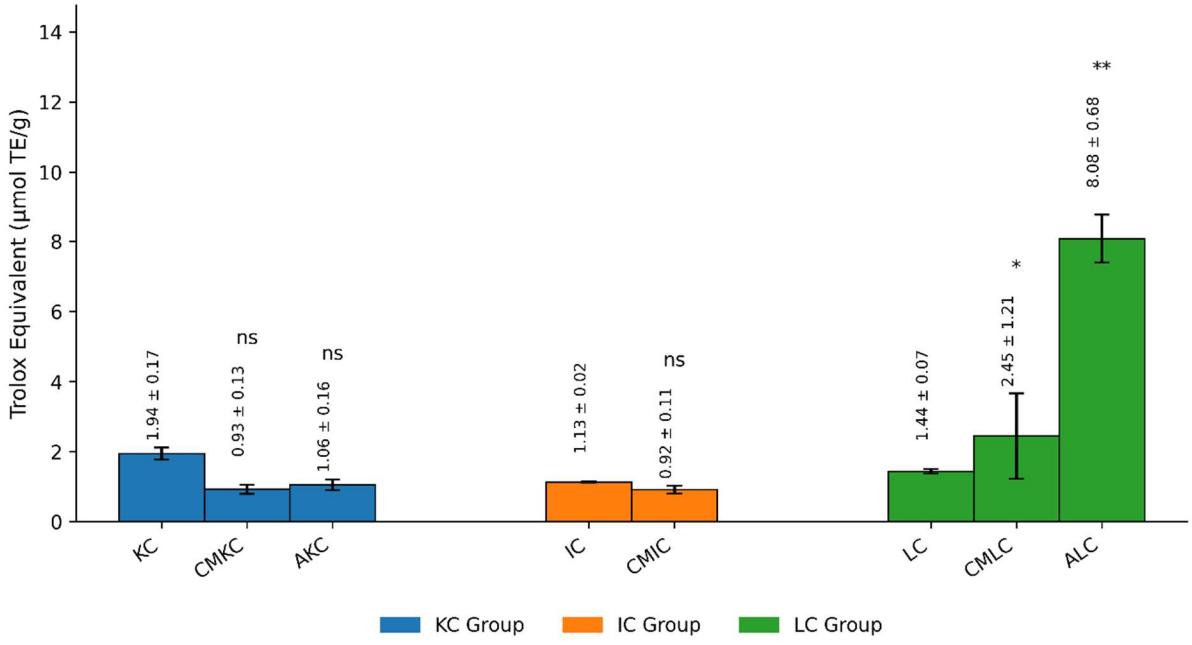

Figure 19: FRAP assay for native and modified carrageenans at 1 mg/mL. * indicates $p < 0.05$ and ** indicates $p < 0.01$, relative to the corresponding unmodified carrageenan.

4.3 Assessing the Degradability of Carrageenan and its Derivatives

4.3.1 Enzymatic Degradation of KC and its Derivatives

In this assay, solutions of the different carrageenan types, their derivatives and glucose standard were incubated with lysozyme (0.01 mg/ml) in a 1:1 ratio in PBS (7.4) at 37 ^{o}C for 10 days. Lysozyme was also applied to glucose because at 0.01 mg/ml lysozyme concentration, partial inhibition of the assay was observed. All polymer solutions were prepared in PBS (pH 7.0), except for ALC, which was dissolved in borate buffer, and chitosan (positive control) , which was dissolved in acetate buffer (pH 5.0).

From table 2, chitosan used as a control showed the greatest amount of degradation by lysozyme, with reducing sugar end groups increasing from 8.26 μg/mL on day 0 to over 167.05 μg/mL by day 10. This validated the activity of lysozyme under the experimental conditions.

For the carrageenan samples, KC showed a steady and gradual increase in degradation products over time, rising from 22.65 μg/mL at day 0 to approximately 65.05 μg/mL at day 10. This indicates that unmodified KC is degradable by lysozyme, likely due to its linear backbone and some level of enzyme accessibility to glycosidic bonds

Interestingly, CMKC showed relatively low degradation among the KC group between day o and day 3. This result suggests that carboxymethylation may reduce enzymatic susceptibility, possibly by introducing steric hindrance or altering chain conformation in a way that blocks lysozyme access. Additionally, the added carboxyl groups could interfere with hydrogen bonding or enzyme binding.

It was observed that for the reducing sugar end release changed from 23.54 μg/mL at day 0 to 79.8 μg/mL at day 3. This change may indicate an early-phase susceptibility due to increased chain mobility or partial backbone disruption introduced during amination.

Table 2: Enzymatic degradation of KC, CMKC and and CMLC at 0.5 mg/mL monitored by pHBH assay (Mean ± SD, *n* = 4). ** $p < 0.01$, 'ns' > 0.05 compared to KC, n.i. indicates no increase after day 3

Sample	Day 0 (μg/mL)	Day 3 (μg/mL)	Day 10 (μg/mL)
Chitosan (CHI)	8.26 ± 4.73	42.73 ± 2.74	167.05 ± 0.10
KC	22.65 ± 11.47	50.94 ± 4.11	65.05 ± 2.68
CMKC	20.44 ± 3.93 ^{ns}	30.98 ± 4.41**	n.i. **
AKC	23.54 ± 6.28 ^{ns}	79.80 ± 1.94**	n.i. **

4.3.2 Enzymatic Degradation of IC and CMIC

For the IC group in table 3, native IC showed relatively low early-stage degradation, with no significant difference in the reducing sugar release through Day 0 and 3, increasing to 94.66 μg/mL on Day 10. This delayed degradation may be attributed to IC's relatively compact helical structure or sulfate content.

CMIC showed a distinct profile: from Day 0 (8.26 μg/mL), degradation rose to 34.77 μg/mL by Day 3 and plateaued by Day 10 (37.93 μg/mL), likely due to steric or electrostatic hindrance from carboxymethyl groups.

Table 3: Enzymatic degradation of IC and CMIC at 0.5 mg/mL monitored by pHBH assay (Mean ± SD, n = 4). ** p< 0.01 compared to IC.

Sample	Day 0 (µg/mL)	Day 3 (µg/mL)	Day 10 (µg/mL)
Chitosan (CHI)	8.26 ± 4.73	42.73 ± 2.74	167.05 ± 0.10
IC	17.32 ± 1.17	16.36 ± 3.72	94.66 ± 7.43
CMIC	8.26 ± 3.93 **	34.77 ± 2.75**	37.93 ± 5.59 **

4.3.3 Enzymatic Degradation of LC and its Derivatives

Among LC and its derivatives shown in table 4, native LC exhibited the highest degradation profile, with reducing sugar ends levels rising from 46.09 µg/mL at Day 0 to 179.44 µg/mL by Day 10 slightly surpassing chitosan. This is notable given that LC is often considered less degradable due to its highly sulfated, branched structure. However, the observed results suggest that LC may possess greater enzyme-accessible regions or higher solubility, which enhances lysozyme interaction under these test conditions.

CMLC followed a similar trend but with slightly lower reducing sugar end release across all timepoints. From 23.54 µg/mL at day 0, degradation increased to 87.89 µg/mL by day 10 . This shows that carboxymethylation partially hinders enzymatic degradation, likely by increasing steric hindrance or reducing the availability of cleavage sites. Nonetheless, the consistent rise in reducing sugar ends equivalents confirms that CMLC remains biodegradable, however at a more moderate rate than native LC.

In contrast, ALC did not show measurable degradation throughout the study period, as reducing sugar ends levels remained near baseline from day 0 to day 10. This suggests that lysozyme activity may be inhibited at the elevated pH of 8.5. Further supporting this, the control using a 1:1 glucose

solution in lysozyme at pH 8.5 under the same conditions also showed no significant change, indicating suppression of lysozyme activity. As expected, glucose alone and glucose with lysozyme behaved the same, confirming that the lack of change was due to enzyme inactivity at this pH.

Table 4: Enzymatic degradation of LC, CMLC and ALC at 0.5 mg/mL monitored by pHBH assay (Mean ± SD, n = 4). ** $p < 0.01$ compared to LC, n.d. indicates not detected.

Sample	Day 0 (μg/mL)	Day 3 (μg/mL)	Day 10 (μg/mL)
Chitosan (CHI)	8.26 ± 4.73	42.73 ± 2.74	167.05 ± 0.10
LC	46.09 ± 3.00	122.14 ± 1.06	179.44 ± 3.4
CMLC	23.54 ± 2.59 **	74.43 ± 9.8**	87.89 ± 11.8 **
ALC	n.d.	n.d.	n.d.

4.4 Antibacterial Activity against Staphylococcus aureus and Pseudomonas aeruginosa

While no growth inhibition was observed by carrageenan and its derivatives against *Pseudomonas aeruginosa*, interesting antibacterial behavior of carrageenans against *Staphylococcus aureus* was observed and discussed below.

4.4.1 Antibacterial Activity of KC, CMKC and AKC against *S. aureus*

In this experiment, PBS served as negative control, gentamicin plus PBS as the positive control for known antibacterial activity, and borate plus PBS as the test control to assess borate's effect on bacterial growth. The antibacterial potential of kappa carrageenan (KC) and its chemically modified derivatives were evaluated against *Staphylococcus aureus* at a fixed concentration of 1 mg/mL across three incubation periods: 4 h, 12 h, and 24 h.

In fig. 20, after 4 hr time point, native KC showed a moderate inhibition of *S. aureus* growth, with a growth inhibition of 35.7%, indicating early antibacterial activity. In contrast, both CMKC (10.0 %) and AKC (4.9 %) showed weaker inhibitory effects at this early stage.

An improvement in bacterial inhibition was observed at 12 h, where all samples showed better inhibition. KC exhibited the highest growth inhibition at 45.9 ± 3.2%, while AKC showed a significant increase to 31.1 ± 3.7%, and CMKC reached 25.1 ± 3.9%. The increase in antibacterial activity with time may be attributed to cumulative damage to the bacterial cell wall or more effective engagement of reactive functional groups in the modified carrageenan chains over time.

At 24 h, KC continued to demonstrate the highest and most consistent inhibition, rising to 53.1 ± 2.8%, suggesting sustained antibacterial efficacy. AKC retained moderate activity (15.8 ± 5.1%), while CMKC's effectiveness diminished to 0.7 ± 5.1%, indicating a possible saturation or neutralization of its functional sites. The reduced activity of CMKC is also likely due to its interaction with the growth environment over time; components of the bacteria or culture media may decrease the availability of CMKC's functional groups, resulting in a weaker response during prolonged incubation.

These findings highlight KC as the most robust antibacterial agent in this group at this concentration and suggest that while chemical modifications may enhance other biofunctionalities (e.g., antioxidant), they do not necessarily improve antibacterial activity in the short-term. The time-dependent nature of inhibition observed for AKC and CMKC underscores the importance of evaluating not just structural modifications, but also their kinetics and stability in biological environments.

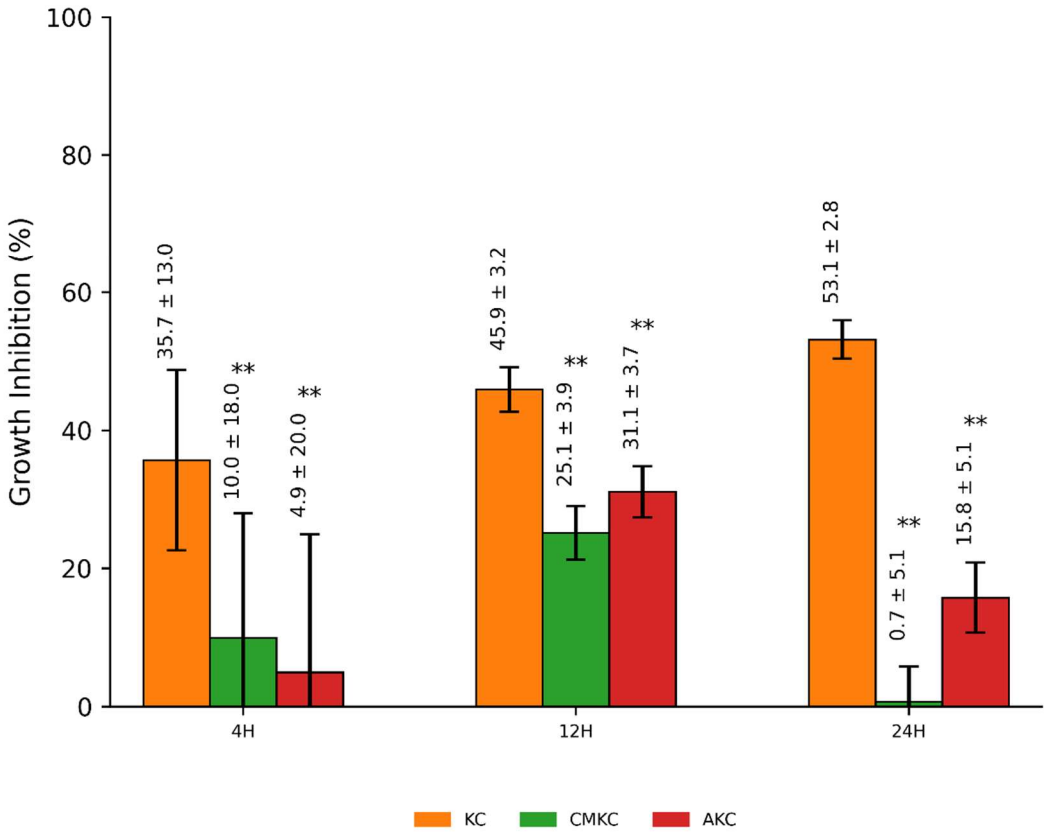

Figure 20: Time-Dependent Growth Inhibition of *Staphylococcus aureus* by KC, CMKC and AKC at 1 mg/mL. ** indicates $p < 0.01$ compared to KC.

4.4.2 Antibacterial Activity of IC and CMIC against *S. aureus*

The antibacterial activities of iota-carrageenan (IC) and its carboxymethylated form (CMIC) were evaluated at 0.25 mg/mL against *Staphylococcus aureus* over 4 and 12 hours.

In fig. 21, CMIC showed higher antibacterial activity, inhibiting bacterial growth by 79.8 ± 4.3% at just 4 hours. This early inhibition suggests effective interaction with bacterial membranes. Although the inhibition slightly decreased to 49.5 ± 5.1% by 12 hours, the activity remained significantly higher than both IC and the PBS control. These results suggest that carboxymethylation of iota carrageenan improves its antibacterial activity possibly by supporting ionic disruption in bacterial cell walls.

In contrast, native IC exhibited weak antibacterial activity at both timepoints, with only 8.9 ± 17.9% inhibition at 4 h and 13.9 ± 5.4% at 12 h.

Taken together, these results support the potential of CMIC as a promising antibacterial polymer against Gram-positive bacteria, capable of exerting rapid and significant inhibition even at lower concentration. The sharp difference between IC and CMIC highlights the importance of carboxymethyl functional groups in modulating biological activity against bacteria.

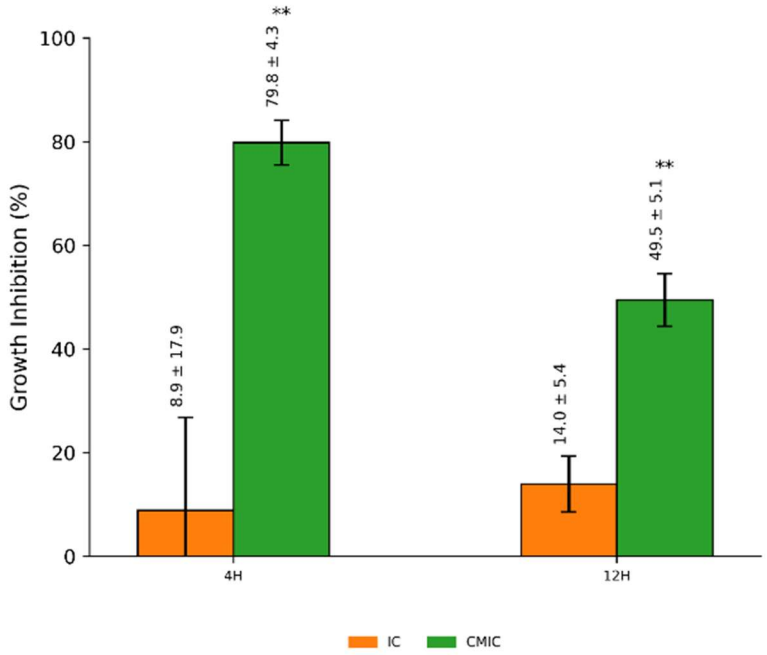

Figure 21: Time-Dependent Growth Inhibition of *Staphylococcus aureus* by IC and CMIC at 0.25 mg/mL. ** indicates $p < 0.01$ compared to IC.

4.4.3 Antibacterial Activity of LC and its Derivatives against *S. aureus*

From fig. 22, lambda-carrageenan (LC) group exhibited distinct antibacterial profiles across its unmodified form and two chemically modified derivatives: carboxymethylated LC (CMLC) and aminated LC (ALC). All samples were tested at 0.25 mg/mL against *Staphylococcus aureus*, with measurements taken at 4, 12, and 24 hours to capture both early and prolonged responses.

At the 4-hour timepoint, both modified carrageenans showed better antibacterial activity than native LC. CMLC achieved 36.7 % growth inhibition and ALC followed with 27.9 %, while LC had only 5.2 %. This suggests that the introduction of carboxymethyl and amine groups increase the antibacterial activity possibly through improved ionic interactions with bacterial membranes. By 12 hours, CMLC showed the highest inhibition at 56.4 ± 2.1%, with ALC reaching 37.0 ± 9.2%, and LC increased to 16.5 ± 4.3%. At the 24-hour, ALC's inhibition increased to 72.1 %. CMLC maintained strong activity (41.6 ± 2.6%), while LC decreased again to 2.4 ± 5.9%, suggesting its limited activity.

It is important to note that growth inhibition values represent the bacterial suppression at each discrete time point rather than cumulative differences between time intervals. Therefore, the time-dependent shifts observed here likely result from dynamic interactions between bacteria and the polymers. *S. aureus* is known to secrete extracellular enzymes such as carrageenases, sulfatases, and glycosidases, which may partially degrade or alter the polysaccharide structure during prolonged incubation. Such enzymatic activity could reduce the charge density or disrupt the polymer conformation, leading to reduced activity as seen for CMLC. Conversely, prolonged incubation may promote further electrostatic adsorption or aggregation of ALC on bacterial surfaces, explaining its strong late-phase inhibition.

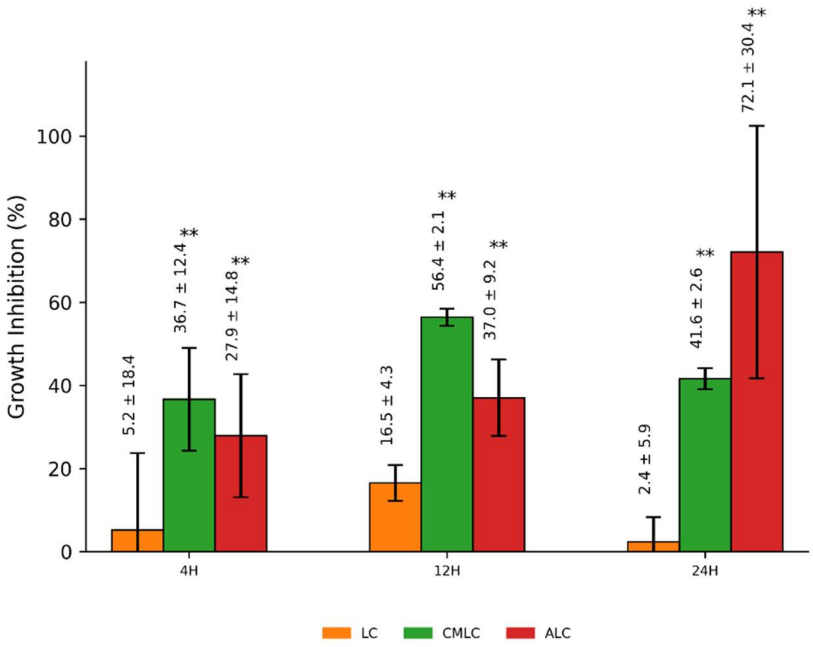

Figure 22: Time-Dependent Growth Inhibition of *Staphylococcus aureus* by LC, CMLC and ALC at 0.25 mg/mL. ** indicates p< 0.01 compared to LC.

4.5 X-ray Photoelectron Spectroscopy (XPS) Analysis of PEM Coatings

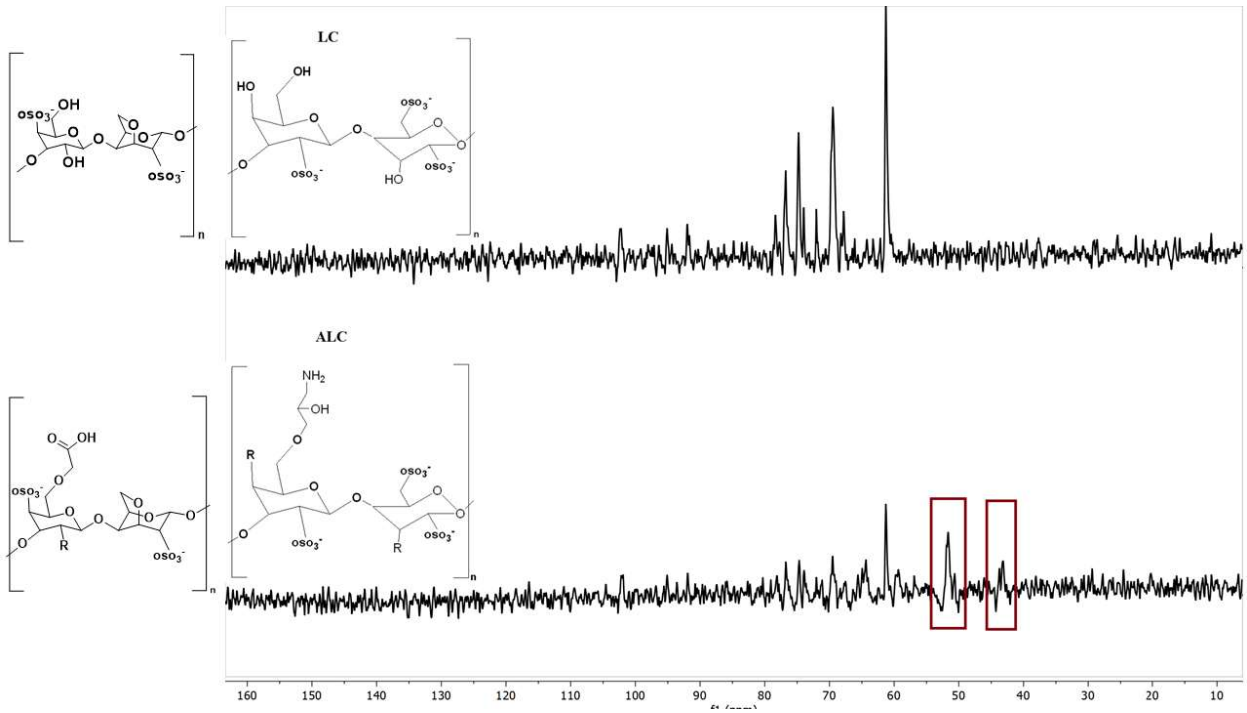

XPS was used to confirm the successful formation of polyelectrolyte multilayers (PEMs) composed of chitosan and modified carrageenans on glass substrates. Figure 23 shows the stacked survey spectra for uncoated glass and for PEMs assembled with carboxymethylated carrageenans (CMKC, CMIC, and CMLC).

The uncoated glass substrate displayed a strong Si 2s/2p signal at approximately 150–105 eV and a smaller O 1s contribution near 530 eV, which are typical of silica surfaces. After PEM deposition, the intensity of the Si peaks disappeared for CMIC and CMLC and markedly decreased for CMKC with atomic percent of ~8 for Si. This indicates coverage of the glass surface by the polyelectrolytes.

For all carrageenan-based PEMs, characteristic peaks corresponding to C 1s (~285 eV) and O 1s (~532 eV) were clearly observed, confirming the presence of chemical elements associated with the polysaccharide layers. Peaks assigned to S 2p (~168 eV) and S 2s (~230 eV) were detected, which originate from the sulfate groups inherent to carrageenans. The appearance of the N 1s (~400 eV) signal in CMKC, CMIC, and CMLC PEMs further supports the incorporation of chitosan to the layers formed.

Overall, the XPS data confirm the successful layer-by-layer assembly of modified carrageenans with chitosan on glass substrates and verify the presence of key chemical elements (C, O, N, and S) associated with the polyelectrolytes.

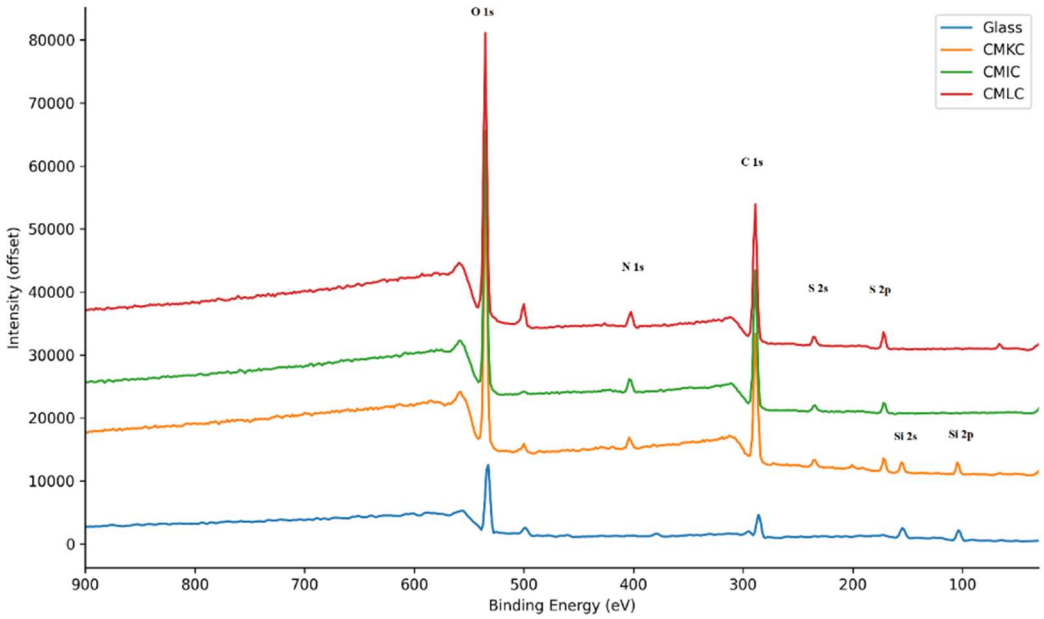

Figure 23: XPS survey spectra of glass substrate, CMKC, CMIC, and CMLC PEMs showing elemental peaks (O 1s, C 1s, N 1s, S 2s/2p, and Si 2s/2p).

4.6 Surface Wettability of PEM Coatings

Water contact angle measurements were performed to assess the surface wettability of the PEMs formed from chitosan and the modified carrageenans. Figure 24 shows that the bare oxidized glass substrate exhibited a contact angle of approximately 68°. Upon deposition of the carrageenan-based multilayers, a decrease in contact angle was observed, confirming successful surface modification and the introduction of hydrophilic functional groups from the polysaccharide coatings.

Among the PEMs, the CMLC film showed a contact angle of 55.2°, while CMIC and CMKC exhibited progressively lower values of 49.7° and 37.8°, respectively. This trend indicates that the degree of hydrophilicity increased with chemical modification and possibly with variations in sulfate and carboxymethyl content across the different carrageenan types. The lower contact angle of CMKC suggests a higher substitution efficiency and lower sulfate content which may be attributed to its denser network of hydrophilic –OH and $–COO^-$.

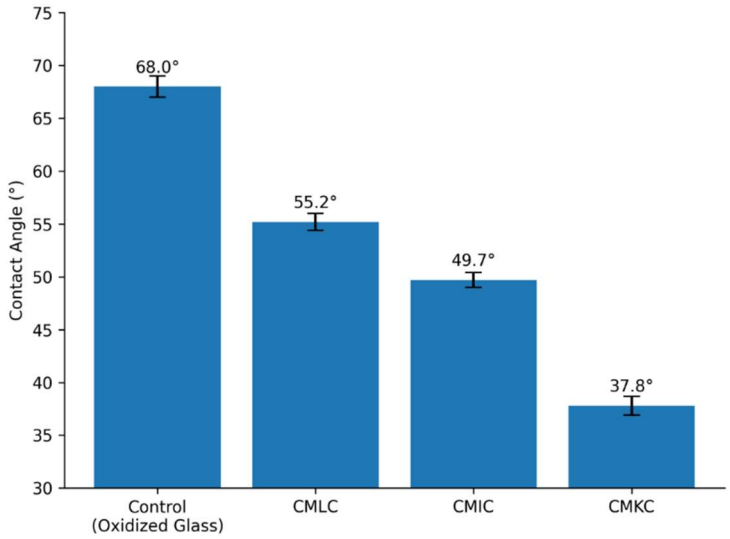

Figure 24: Water contact angles of carboxymethylated carrageenan coatings on glass substrate.

Together with the XPS results, the water contact angle data provides evidence of successful PEM assembly and demonstrates how the surface wettability can be tuned by varying the carrageenan type and degree of modification.

4.7 Atomic Force Microscopy of PEMs and Surface Degraded PEMs

To understand the stability of PEMs made using carboxymethylated kappa and iota carrageenans as polyanions and chitosan as polycations, these PEMs were incubated at room temperature in PBS (pH 7.4) containing lysozyme at 0.25 mg/mL for 21 days (n = 3). The surfaces of these coatings were then analyzed with an atomic force microscope and the image is shown in fig 25. The mean arithmetic roughness (Ra) of CMKC PEMs increased from 10.9 nm to 15.1 nm, while that of CMIC changed from 10.4 nm to 12.5 nm after the 21-day incubation period. This progressive increase in roughness indicates that lysozyme may enzymatically cleave and disrupt the polysaccharide chains within the PEM surface, causing gradual degradation and altered surface topography over time.

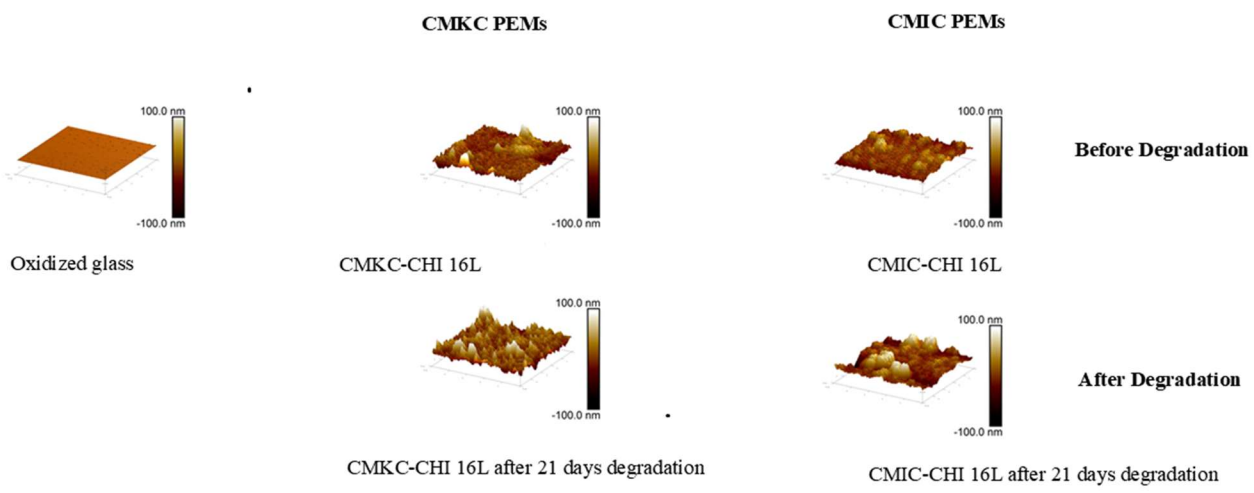

Figure 25: 5 µm × 5 µm AFM height images of layer-by-layer assembled PEMs on oxidized glass.

5.0 Conclusion

This study explored the chemical modification of kappa, iota and lambda carrageenans to create multifunctional polysaccharides for biomedical surface applications. Through carboxymethylation and several amination strategies, we successfully introduced additional functional groups to alter reactivity, and biological performance. These modifications were confirmed through structural characterization and tested across a series of biological and material performance assays.

Antioxidant activity, as evaluated using DPPH, ABTS, and FRAP assays, revealed that modified carrageenans exhibited significantly radical scavenging properties compared to their unmodified counterparts. This change can be attributed to the increased or decreased availability of electron-

donating groups introduced during modification, particularly the presence of free amines and carboxylic acids.

Antibacterial activity was studied against both Gram-positive (*Staphylococcus aureus*) and Gram-negative (*Pseudomonas aeruginosa*) bacteria using the broth microdilution method. While no inhibition against *Pseudomonas aeruginosa* was observed*, the* results for *Staphylococcus aureus* demonstrated that certain modified carrageenans, especially CMIC and CMKC, inhibited bacterial growth more effectively than their native forms at the conditions considered. These findings suggest a correlation between chemically modified carrageenan and antibacterial behavior, with amine-rich derivatives showing enhanced interaction with negatively charged bacterial membranes.

Enzymatic degradation using lysozyme provided insights into the stability and biodegradability of the modified polysaccharides. In solution, the release of reducing sugars over a 10-day period demonstrated that modification does not completely inhibit degradation, although susceptibility varies across derivatives. Surface degradation studies of PEMs further confirmed structural changes, with AFM revealing change in surface topography over time. The successful use of the pHBH assay to quantify degradation products offers a simple, reproducible approach for monitoring polysaccharide breakdown.

Using the layer-by-layer (LbL) technique, polyelectrolyte multilayers (PEMs) were fabricated on glass substrates with chitosan as the polycation and the modified carrageenans as the polyanions. The build-up of 16-layer PEMs was achieved reliably, and surface characterization confirmed uniform deposition and controlled thickness.

Collectively, this research demonstrates that tailored chemical modification of carrageenans can significantly enhance their functional properties, making them promising candidates for

multifunctional biomedical coatings. Their bioactivity, biodegradability, and compatibility with established surface engineering techniques position them as viable alternatives to synthetic and animal-derived polymers, such as heparin.

6.0 Bibliography

1. Ahmad, M. M. (2021). Recent trends in chemical modification and antioxidant activities of plants-based polysaccharides: A review. *Carbohydrate Polymer Technologies and Applications*, *2*, 100045. https://doi.org/10.1016/j.carpta.2021.100045
2. Ahmad Raus, R., Wan Nawawi, W. M. F., & Nasaruddin, R. R. (2021). Alginate and alginate composites for biomedical applications. *Asian Journal of Pharmaceutical Sciences*, *16*(3), 280–306. https://doi.org/10.1016/j.ajps.2020.10.001
3. Ahmadabadi, H. Y., Yu, K., & Kizhakkedathu, J. N. (2020). Surface modification approaches for prevention of implant associated infections. *Colloids and Surfaces B: Biointerfaces*, *193*, 111116. https://doi.org/10.1016/j.colsurfb.2020.111116

4. Almodóvar, J., Place, L. W., Gogolski, J., Erickson, K., & Kipper, M. J. (2011). Layer-by-Layer Assembly of Polysaccharide-Based Polyelectrolyte Multilayers: A Spectroscopic Study of Hydrophilicity, Composition, and Ion Pairing. *Biomacromolecules*, *12*(7), 2755–2765. https://doi.org/10.1021/bm200519y
5. Aparna, V., Melge, A. R., Rajan, V. K., Biswas, R., Jayakumar, R., & Gopi Mohan, C. (2018). Carboxymethylated ι-carrageenan conjugated amphotericin B loaded gelatin nanoparticles for treating intracellular Candida glabrata infections. *International Journal of Biological Macromolecules*, *110*, 140–149. https://doi.org/10.1016/j.ijbiomac.2017.11.126
6. Arciola, C. R., Campoccia, D., & Montanaro, L. (2018a). Implant infections: Adhesion, biofilm formation and immune evasion. *Nature Reviews Microbiology*, *16*(7), 397–409. https://doi.org/10.1038/s41579-018-0019-y
7. Arciola, C. R., Campoccia, D., & Montanaro, L. (2018b). Implant infections: Adhesion, biofilm formation and immune evasion. *Nature Reviews Microbiology*, *16*(7), 397–409. https://doi.org/10.1038/s41579-018-0019-y
8. Arciola, C. R., Campoccia, D., Speziale, P., Montanaro, L., & Costerton, J. W. (2012). Biofilm formation in Staphylococcus implant infections. A review of molecular mechanisms and implications for biofilm-resistant materials. *Biomaterials*, *33*(26), 5967–5982. https://doi.org/10.1016/j.biomaterials.2012.05.031
9. Arlov, Ø., Rütsche, D., Asadi Korayem, M., Öztürk, E., & Zenobi-Wong, M. (2021). Engineered Sulfated Polysaccharides for Biomedical Applications. *Advanced Functional Materials*, *31*(19), 2010732. https://doi.org/10.1002/adfm.202010732

10. Bădilă, A. E., Rădulescu, D. M., Ilie, A., Niculescu, A.-G., Grumezescu, A. M., & Rădulescu, A. R. (2022). Bone Regeneration and Oxidative Stress: An Updated Overview. *Antioxidants*, *11*(2), 318. https://doi.org/10.3390/antiox11020318
11. Biran, R., & Pond, D. (2017). Heparin coatings for improving blood compatibility of medical devices. *Advanced Drug Delivery Reviews*, *112*, 12–23. https://doi.org/10.1016/j.addr.2016.12.002
12. Boddohi, S., Almodóvar, J., Zhang, H., Johnson, P. A., & Kipper, M. J. (2010). Layer-by-layer assembly of polysaccharide-based nanostructured surfaces containing polyelectrolyte complex nanoparticles. *Colloids and Surfaces B: Biointerfaces*, *77*(1), 60–68. https://doi.org/10.1016/j.colsurfb.2010.01.006
13. Bohara, S., & Suthakorn, J. (2022a). Surface coating of orthopedic implant to enhance the osseointegration and reduction of bacterial colonization: A review. *Biomaterials Research*, *26*(1), 26. https://doi.org/10.1186/s40824-022-00269-3
14. Bohara, S., & Suthakorn, J. (2022b). Surface coating of orthopedic implant to enhance the osseointegration and reduction of bacterial colonization: A review. *Biomaterials Research*, *26*(1), 26. https://doi.org/10.1186/s40824-022-00269-3
15. Castilla-Casadiego, D. A., Pinzon-Herrera, L., Perez-Perez, M., Quiñones-Colón, B. A., Suleiman, D., & Almodovar, J. (2018). Simultaneous characterization of physical, chemical, and thermal properties of polymeric multilayers using infrared spectroscopic ellipsometry. *Colloids and Surfaces A: Physicochemical and Engineering Aspects*, *553*, 155–168. https://doi.org/10.1016/j.colsurfa.2018.05.052

16. Chae, K., Jang, W. Y., Park, K., Lee, J., Kim, H., Lee, K., Lee, C. K., Lee, Y., Lee, S. H., & Seo, J. (2020a). Antibacterial infection and immune-evasive coating for orthopedic implants. *Science Advances*, *6*(44), eabb0025. https://doi.org/10.1126/sciadv.abb0025
17. Chae, K., Jang, W. Y., Park, K., Lee, J., Kim, H., Lee, K., Lee, C. K., Lee, Y., Lee, S. H., & Seo, J. (2020b). Antibacterial infection and immune-evasive coating for orthopedic implants. *Science Advances*, *6*(44), eabb0025. https://doi.org/10.1126/sciadv.abb0025
18. Collén, P. N., Lemoine, M., Daniellou, R., Guégan, J.-P., Paoletti, S., & Helbert, W. (2009). Enzymatic Degradation of κ-Carrageenan in Aqueous Solution. *Biomacromolecules*, *10*(7), 1757–1767. https://doi.org/10.1021/bm9001766
19. Cuker, A., Arepally, G. M., Chong, B. H., Cines, D. B., Greinacher, A., Gruel, Y., Linkins, L. A., Rodner, S. B., Selleng, S., Warkentin, T. E., Wex, A., Mustafa, R. A., Morgan, R. L., & Santesso, N. (2018). American Society of Hematology 2018 guidelines for management of venous thromboembolism: Heparin-induced thrombocytopenia. *Blood Advances*, *2*(22), 3360–3392. https://doi.org/10.1182/bloodadvances.2018024489
20. Das, I. J., & Bal, T. (2024). Exploring carrageenan: From seaweed to biomedicine—A comprehensive review. *International Journal of Biological Macromolecules*, *268*, 131822. https://doi.org/10.1016/j.ijbiomac.2024.131822
21. De Araújo, C. A., Noseda, M. D., Cipriani, T. R., Gonçalves, A. G., Duarte, M. E. R., & Ducatti, D. R. B. (2013). Selective sulfation of carrageenans and the influence of sulfate regiochemistry on anticoagulant properties. *Carbohydrate Polymers*, *91*(2), 483–491. https://doi.org/10.1016/j.carbpol.2012.08.034
22. Dedhia, N. J., Marathe, S. J., & Singhal, R. S. (2021). Amine Modification. In H. H. Gahruie, M. H. Eskandari, A. Mousavi Khaneghah, & F. Ghiasi (Eds.), *Physicochemical*

and Enzymatic Modification of Gums (pp. 111–133). Springer International Publishing. https://doi.org/10.1007/978-3-030-87996-9_6

23. D'Este, M., Eglin, D., & Alini, M. (2014). A systematic analysis of DMTMM vs EDC/NHS for ligation of amines to Hyaluronan in water. *Carbohydrate Polymers*, *108*, 239–246. https://doi.org/10.1016/j.carbpol.2014.02.070
24. Dudonné, S., Vitrac, X., Coutière, P., Woillez, M., & Mérillon, J.-M. (2009). Comparative Study of Antioxidant Properties and Total Phenolic Content of 30 Plant Extracts of Industrial Interest Using DPPH, ABTS, FRAP, SOD, and ORAC Assays. *Journal of Agricultural and Food Chemistry*, *57*(5), 1768–1774. https://doi.org/10.1021/jf803011r
25. Esquivel-Chirino, C., Gómez-Landeros, J. C., Carabantes-Campos, E. P., Carmona-Ruiz, D., Valero-Princet, Y., Márquez-Correa, C., & Morales-González, J. A. (2021). The Impact of Oxidative Stress on Dental Implants. *European Journal of Dental and Oral Health*, *2*(1), 1–8. https://doi.org/10.24018/ejdent.2021.2.1.37
26. Fadzil, A. F. B. A., Pramanik, A., Basak, A. K., Prakash, C., & Shankar, S. (2022). Role of surface quality on biocompatibility of implants—A review. *Annals of 3D Printed Medicine*, *8*, 100082. https://doi.org/10.1016/j.stlm.2022.100082
27. Fatima, R., Prasher, P., Sharma, M., Chellappan, D. K., Gupta, G., Singh, S. K., Patravale, V. B., & Dua, K. (2023). Aminated Polysaccharides: Unveiling a new frontier for enhanced therapeutic efficacy. *Journal of Drug Delivery Science and Technology*, *89*, 105090. https://doi.org/10.1016/j.jddst.2023.105090
28. Fischer, N. G., Chen, X., Astleford-Hopper, K., He, J., Mullikin, A. F., Mansky, K. C., & Aparicio, C. (2021). Antimicrobial and enzyme-responsive multi-peptide surfaces for

bone-anchored devices. *Materials Science and Engineering: C*, *125*, 112108. https://doi.org/10.1016/j.msec.2021.112108

29. Galliera, E., Massaccesi, L., Banfi, G., De Vecchi, E., Ragone, V., & Corsi Romanelli, M. M. (2021a). Effect of Oxidative Stress on Bone Remodeling in Periprosthetic Osteolysis. *Clinical Reviews in Bone and Mineral Metabolism*, *19*(1–4), 14–23. https://doi.org/10.1007/s12018-021-09278-7
30. Galliera, E., Massaccesi, L., Banfi, G., De Vecchi, E., Ragone, V., & Corsi Romanelli, M. M. (2021b). Effect of Oxidative Stress on Bone Remodeling in Periprosthetic Osteolysis. *Clinical Reviews in Bone and Mineral Metabolism*, *19*(1–4), 14–23. https://doi.org/10.1007/s12018-021-09278-7
31. Gronbeck, C., Cusano, A., Cardenas, J. M., Harrington, M. A., & Halawi, M. J. (2020). Primary Total Hip Arthroplasty in Hispanic/Latino Patients: An Updated Nationwide Analysis of Length of Stay, 30-Day Outcomes, and Risk Factors. *Arthroplasty Today*, *6*(4), 721–725. https://doi.org/10.1016/j.artd.2020.07.035
32. Gupta, V. (2001). Controlled-release tablets from carrageenans: Effect of formulation, storage and dissolution factors. *European Journal of Pharmaceutics and Biopharmaceutics*, *51*(3), 241–248. https://doi.org/10.1016/S0939-6411(01)00135-7
33. Hameister, R., Kaur, C., Dheen, S. T., Lohmann, C. H., & Singh, G. (2020). Reactive oxygen/nitrogen species (ROS/RNS) and oxidative stress in arthroplasty. *Journal of Biomedical Materials Research Part B: Applied Biomaterials*, *108*(5), 2073–2087. https://doi.org/10.1002/jbm.b.34546
34. Hedlund, K., Coyne, D., Sanford, D., & Huddelson, J. (2013). The heparin recall of 2008. *Perfusion*, *28*(1), 61–65. https://doi.org/10.1177/0267659112462274

35. Humayun, S., Premarathna, A. D., Rjabovs, V., Howlader, M. M., Darko, C. N. S., Mok, I.-K., & Tuvikene, R. (2023). Biochemical Characteristics and Potential Biomedical Applications of Hydrolyzed Carrageenans. *Marine Drugs*, *21*(5), 269. https://doi.org/10.3390/md21050269

36. Huzum, B., Puha, B., Necoara, R., Gheorghevici, S., Puha, G., Filip, A., Sirbu, P., & Alexa, O. (2021). Biocompatibility assessment of biomaterials used in orthopedic devices: An overview (Review). *Experimental and Therapeutic Medicine*, *22*(5), 1315. https://doi.org/10.3892/etm.2021.10750

37. Infection and Your Hip Replacement. (n.d.). *AAHKS*. Retrieved September 22, 2025, from https://hipkneeinfo.org/hip-care/infection-and-your-joint-replacement/

38. Inui, H., Yamagami, R., Kono, K., & Kawaguchi, K. (2023). What are the causes of failure after total knee arthroplasty? *Journal of Joint Surgery and Research*, *1*(1), 32–40. https://doi.org/10.1016/j.jjoisr.2022.12.002

39. Izumrudov, V. A., Mussabayeva, B. Kh., & Murzagulova, K. B. (2018). Polyelectrolyte multilayers: Preparation and applications. *Russian Chemical Reviews*, *87*(2), 192–200. https://doi.org/10.1070/RCR4767

40. Jin, W., & Chu, P. K. (2019). Orthopedic Implants. In *Encyclopedia of Biomedical Engineering* (pp. 425–439). Elsevier. https://doi.org/10.1016/B978-0-12-801238-3.10999-7

41. Joshi, M. U., Kulkarni, S. P., Choppadandi, M., Keerthana, M., & Kapusetti, G. (2023). Current state of art smart coatings for orthopedic implants: A comprehensive review. *Smart Materials in Medicine*, *4*, 661–679. https://doi.org/10.1016/j.smaim.2023.06.005

42. Jumaah, F. N., Mobarak, N. N., Ahmad, A., Ghani, M. A., & Rahman, M. Y. A. (2015). Derivative of iota-carrageenan as solid polymer electrolyte. *Ionics*, *21*(5), 1311–1320. https://doi.org/10.1007/s11581-014-1306-x

43. Kalpana Manivannan, R., Sharma, N., Kumar, V., Jayaraj, I., Vimal, S., & Umesh, M. (2024). A comprehensive review on natural macromolecular biopolymers for biomedical applications: Recent advancements, current challenges, and future outlooks. *Carbohydrate Polymer Technologies and Applications*, *8*, 100536. https://doi.org/10.1016/j.carpta.2024.100536

44. Kim, J. H., Lee, J., Park, J., & Gho, Y. S. (2015). Gram-negative and Gram-positive bacterial extracellular vesicles. *Seminars in Cell & Developmental Biology*, *40*, 97–104. https://doi.org/10.1016/j.semcdb.2015.02.006

45. Kravanja, K. A., & Finšgar, M. (2021). Analytical Techniques for the Characterization of Bioactive Coatings for Orthopaedic Implants. *Biomedicines*, *9*(12), 1936. https://doi.org/10.3390/biomedicines9121936

46. Kumar, M., Kumar, R., & Kumar, S. (2021). Coatings on orthopedic implants to overcome present problems and challenges: A focused review. *Materials Today: Proceedings*, *45*, 5269–5276. https://doi.org/10.1016/j.matpr.2021.01.831

47. Kumar, S., Bhatt, A., & Purohit, P. (2025). Carrageenan Modifications: Improving Biomedical Applications. *Journal of Polymers and the Environment*, *33*(4), 1667–1688. https://doi.org/10.1007/s10924-025-03501-y

48. Kunutsor, S. K., Beswick, A. D., Whitehouse, M. R., Wylde, V., & Blom, A. W. (2018). Debridement, antibiotics and implant retention for periprosthetic joint infections: A

systematic review and meta-analysis of treatment outcomes. *Journal of Infection*, *77*(6), 479–488. https://doi.org/10.1016/j.jinf.2018.08.017

49. Kuznetsova, T. A., Andryukov, B. G., Makarenkova, I. D., Zaporozhets, T. S., Besednova, N. N., Fedyanina, L. N., Kryzhanovsky, S. P., & Shchelkanov, M. Yu. (2021). The Potency of Seaweed Sulfated Polysaccharides for the Correction of Hemostasis Disorders in COVID-19. *Molecules*, *26*(9), 2618. https://doi.org/10.3390/molecules26092618
50. Labafzadeh, S. R., Vyavaharkar, K., Kavakka, J. S., King, A. W. T., & Kilpeläinen, I. (2015). Amination and thiolation of chloroacetyl cellulose through reactive dissolution in N,N-dimethylformamide. *Carbohydrate Polymers*, *116*, 60–66. https://doi.org/10.1016/j.carbpol.2014.03.077
51. Leong, K. H., Chung, L. Y., Noordin, M. I., Mohamad, K., Nishikawa, M., Onuki, Y., Morishita, M., & Takayama, K. (2011). Carboxymethylation of kappa-carrageenan for intestinal-targeted delivery of bioactive macromolecules. *Carbohydrate Polymers*, *83*(4), 1507–1515. https://doi.org/10.1016/j.carbpol.2010.09.062
52. Lewallen, E. A., Riester, S. M., Bonin, C. A., Kremers, H. M., Dudakovic, A., Kakar, S., Cohen, R. C., Westendorf, J. J., Lewallen, D. G., & Van Wijnen, A. J. (2015). Biological Strategies for Improved Osseointegration and Osteoinduction of Porous Metal Orthopedic Implants. *Tissue Engineering Part B: Reviews*, *21*(2), 218–230. https://doi.org/10.1089/ten.teb.2014.0333
53. Li, C., Hein, S., & Wang, K. (2013). Chitosan-Carrageenan Polyelectrolyte Complex for the Delivery of Protein Drugs. *ISRN Biomaterials*, *2013*, 1–6. https://doi.org/10.5402/2013/629807

54. Li, L., Ni, R., Shao, Y., & Mao, S. (2014). Carrageenan and its applications in drug delivery. *Carbohydrate Polymers*, *103*, 1–11. https://doi.org/10.1016/j.carbpol.2013.12.008

55. Liang, W., Mao, X., Peng, X., & Tang, S. (2014). Effects of sulfate group in red seaweed polysaccharides on anticoagulant activity and cytotoxicity. *Carbohydrate Polymers*, *101*, 776–785. https://doi.org/10.1016/j.carbpol.2013.10.010

56. Loukelis, K., Papadogianni, D., & Chatzinikolaidou, M. (2022). Kappa-carrageenan/chitosan/gelatin scaffolds enriched with potassium chloride for bone tissue engineering. *International Journal of Biological Macromolecules*, *209*, 1720–1730. https://doi.org/10.1016/j.ijbiomac.2022.04.129

57. Lyu, S., & Untereker, D. (2009). Degradability of Polymers for Implantable Biomedical Devices. *International Journal of Molecular Sciences*, *10*(9), 4033–4065. https://doi.org/10.3390/ijms10094033

58. Madruga, L. Y. C., Baghersad, S., Câmara, P. C. F., Sabino, R. M., Kipper, M. J., & Popat, K. C. (2025). *Carboxymethyl kappa-carrageenan polyelectrolyte multilayers: Anticoagulant blood-compatible coatings as sustainable alternatives to heparin for blood-contacting surfaces*. In Review. https://doi.org/10.21203/rs.3.rs-7014360/v1

59. Madruga, L. Y. C., Sabino, R. M., Santos, E. C. G., Popat, K. C., Balaban, R. D. C., & Kipper, M. J. (2020). Carboxymethyl-kappa-carrageenan: A study of biocompatibility, antioxidant and antibacterial activities. *International Journal of Biological Macromolecules*, *152*, 483–491. https://doi.org/10.1016/j.ijbiomac.2020.02.274

60. Malyarenko, O. S., Usoltseva, R. V., Silchenko, A. S., & Ermakova, S. P. (2020). Aminated laminaran from brown alga Saccharina cichorioides: Synthesis, structure, anticancer, and

radiosensitizing potential in vitro. *Carbohydrate Polymers*, *250*, 117007. https://doi.org/10.1016/j.carbpol.2020.117007

61. Mastnak, T., Maver, U., & Finšgar, M. (2022). Addressing the Needs of the Rapidly Aging Society through the Development of Multifunctional Bioactive Coatings for Orthopedic Applications. *International Journal of Molecular Sciences*, *23*(5), 2786. https://doi.org/10.3390/ijms23052786
62. Mitchell, S. (2020, April 13). XPS Analysis of Surface Modified Polymers. *EAG Laboratories*. https://www.eag.com/app-note/xps-analysis-of-surface-modified-polymers/
63. Mokhtari, H., Tavakoli, S., Safarpour, F., Kharaziha, M., Bakhsheshi-Rad, H. R., Ramakrishna, S., & Berto, F. (2021). *Recent advances in chemically-modified and hybrid carrageenan-based platforms for drug delivery, wound healing, and tissue engineering*. https://scholarbank.nus.edu.sg/handle/10635/232075
64. Nathanael, A. J., & Oh, T. H. (2020). Biopolymer Coatings for Biomedical Applications. *Polymers*, *12*(12), 3061. https://doi.org/10.3390/polym12123061
65. Neamtu, B., Barbu, A., Negrea, M. O., Berghea-Neamțu, C. Ștefan, Popescu, D., Zăhan, M., & Mireșan, V. (2022). Carrageenan-Based Compounds as Wound Healing Materials. *International Journal of Molecular Sciences*, *23*(16), 9117. https://doi.org/10.3390/ijms23169117
66. Necas, J., & Bartosikova, L. (2013). Carrageenan: A review. *Veterinární Medicína*, *58*(4), 187–205. https://doi.org/10.17221/6758-VETMED
67. *Orthopedic Implants Market Size | Industry Report, 2030*. (n.d.). Retrieved September 22, 2025, from https://www.grandviewresearch.com/industry-analysis/orthopedic-implants-market

68. Pacheco-Quito, E.-M., Ruiz-Caro, R., & Veiga, M.-D. (2020). Carrageenan: Drug Delivery Systems and Other Biomedical Applications. *Marine Drugs*, *18*(11), 583. https://doi.org/10.3390/md18110583

69. Pires, P. C., Mascarenhas-Melo, F., Pedrosa, K., Lopes, D., Lopes, J., Macário-Soares, A., Peixoto, D., Giram, P. S., Veiga, F., & Paiva-Santos, A. C. (2023). Polymer-based biomaterials for pharmaceutical and biomedical applications: A focus on topical drug administration. *European Polymer Journal*, *187*, 111868. https://doi.org/10.1016/j.eurpolymj.2023.111868

70. Ricciardi, G., Siracusano, L., Micale, E., Addorisio, V., Ballato, M., Donadio, D., Tralongo, P., Giuffrè, G., Leonetti, D., Martini, M., & Zampogna, B. (2025). Aseptic Loosening in Total Hip Arthroplasty: Pathophysiology, Biomarkers, and Preventive Treatment Strategies. *Applied Sciences*, *15*(16), 9156. https://doi.org/10.3390/app15169156

71. Rupert, R., Rodrigues, K. F., Thien, V. Y., & Yong, W. T. L. (2022). Carrageenan From Kappaphycus alvarezii (Rhodophyta, Solieriaceae): Metabolism, Structure, Production, and Application. *Frontiers in Plant Science*, *13*, 859635. https://doi.org/10.3389/fpls.2022.859635

72. Sargison, L., Smith, R. A. A., Carnachan, S. M., Daines, A. M., Brackovic, A., Kidgell, J. T., Nurcombe, V., Cool, S. M., Sims, I. M., & Hinkley, S. F. R. (2022). Variability in the composition of porcine mucosal heparan sulfates. *Carbohydrate Polymers*, *282*, 119081. https://doi.org/10.1016/j.carbpol.2021.119081

73. Schierholz, J. M., & Beuth, J. (2001). Implant infections: A haven for opportunistic bacteria. *Journal of Hospital Infection*, *49*(2), 87–93. https://doi.org/10.1053/jhin.2001.1052

74. Seetharaman, S., Sankaranarayanan, D., & Gupta, M. (2023). Magnesium-Based Temporary Implants: Potential, Current Status, Applications, and Challenges. *Journal of Functional Biomaterials*, *14*(6), 324. https://doi.org/10.3390/jfb14060324

75. Setz, C., Große, M., Fröba, M., Auth, J., Rauch, P., Herrmann, A., Cordsmeier, A., Ensser, A., Schindler, M., Morokutti-Kurz, M., Graf, P., Engel, B., Prieschl-Grassauer, E., Grassauer, A., & Schubert, U. (2023). Iota-Carrageenan Inhibits Replication of the SARS-CoV-2 Variants of Concern Omicron BA.1, BA.2 and BA.5. *Nutraceuticals*, *3*(3), 315–328. https://doi.org/10.3390/nutraceuticals3030025

76. Soeda, S., Ishida, S., Honda, O., Shimeno, H., & Nagamatsu, A. (1994). Aminated fucoidan promotes the invasion of 3 LL cells through reconstituted basement membrane: Its possible mechanism of action. *Cancer Letters*, *85*(1), 133–138. https://doi.org/10.1016/0304-3835(94)90249-6

77. Song, X., Wang, K., Tang, C.-Q., Yang, W.-W., Zhao, W.-F., & Zhao, C.-S. (2018). Design of Carrageenan-Based Heparin-Mimetic Gel Beads as Self-Anticoagulant Hemoperfusion Adsorbents. *Biomacromolecules*, *19*(6), 1966–1978. https://doi.org/10.1021/acs.biomac.7b01724

78. Supra, R., & K Agrawal, D. (2023). Innate Immune Response in Orthopedic Implant Failure. *Journal of Orthopaedics and Sports Medicine*, *05*(01). https://doi.org/10.26502/josm.511500073

79. Tavakoli, S., Kharaziha, M., Kermanpur, A., & Mokhtari, H. (2019). Sprayable and injectable visible-light Kappa-carrageenan hydrogel for in-situ soft tissue engineering. *International Journal of Biological Macromolecules*, *138*, 590–601. https://doi.org/10.1016/j.ijbiomac.2019.07.126

80. Tavares, T. D., Antunes, J. C., Padrão, J., Ribeiro, A. I., Zille, A., Amorim, M. T. P., Ferreira, F., & Felgueiras, H. P. (2020). Activity of Specialized Biomolecules against Gram-Positive and Gram-Negative Bacteria. *Antibiotics*, *9*(6), 314. https://doi.org/10.3390/antibiotics9060314

81. Tian, R., Li, K., Lin, Y., Lu, C., & Duan, X. (2023). Characterization Techniques of Polymer Aging: From Beginning to End. *Chemical Reviews*, *123*(6), 3007–3088. https://doi.org/10.1021/acs.chemrev.2c00750

82. Troy, E., Tilbury, M. A., Power, A. M., & Wall, J. G. (2021). Nature-Based Biomaterials and Their Application in Biomedicine. *Polymers*, *13*(19), 3321. https://doi.org/10.3390/polym13193321

83. Vahabzadeh, S., Roy, M., Bandyopadhyay, A., & Bose, S. (2015). Phase stability and biological property evaluation of plasma sprayed hydroxyapatite coatings for orthopedic and dental applications. *Acta Biomaterialia*, *17*, 47–55. https://doi.org/10.1016/j.actbio.2015.01.022

84. Villegas, M., Bayat, F., Kramer, T., Schwarz, E., Wilson, D., Hosseinidoust, Z., & Didar, T. (2023). *Strategies to Prevent Bacterial Infections on Titanium-Based Orthopedic and Dental Implants*. Chemistry. https://doi.org/10.26434/chemrxiv-2023-zjb5t

85. Vishnu, J., Kesavan, P., Shankar, B., Dembińska, K., Swiontek Brzezinska, M., & Kaczmarek-Szczepańska, B. (2023). Engineering Antioxidant Surfaces for Titanium-Based Metallic Biomaterials. *Journal of Functional Biomaterials*, *14*(7), 344. https://doi.org/10.3390/jfb14070344

86. Vlcek, J. R., Reynolds, M. M., & Kipper, M. J. (2021). Enzymatic Degradation of Glycosaminoglycans and Proteoglycan-Mimetic Materials in Solution and on

Polyelectrolyte Multilayer Surfaces. *Biomacromolecules*, *22*(9), 3913–3925. https://doi.org/10.1021/acs.biomac.1c00720

87. Volpin, A., Sukeik, M., Alazzawi, S., & Haddad, F. S. (2016). Aggressive Early Debridement in Treatment of Acute Periprosthetic Joint Infections After Hip and Knee Replacements. *The Open Orthopaedics Journal*, *10*(1), 669–678. https://doi.org/10.2174/1874325001610010669
88. Wang, J., Zhang, Q., Zhang, Z., Zhang, J., & Li, P. (2009). Synthesized phosphorylated and aminated derivatives of fucoidan and their potential antioxidant activity in vitro. *International Journal of Biological Macromolecules*, *44*(2), 170–174. https://doi.org/10.1016/j.ijbiomac.2008.11.010
89. Wang, M., & Tang, T. (2019). Surface treatment strategies to combat implant-related infection from the beginning. *Journal of Orthopaedic Translation*, *17*, 42–54. https://doi.org/10.1016/j.jot.2018.09.001
90. Xia, B., Liu, Y., Xing, Y., Shi, Z., & Pan, X. (2025). Biodegradable Medical Implants: Reshaping Future Medical Practice. *Advanced Science*, *12*(35), e08014. https://doi.org/10.1002/advs.202508014
91. Yan, Y., Neville, A., & Dowson, D. (2007). Tribo-corrosion properties of cobalt-based medical implant alloys in simulated biological environments. *Wear*, *263*(7–12), 1105–1111. https://doi.org/10.1016/j.wear.2007.01.114
92. Yang, J., Liu, C., Sun, H., Liu, Y., Liu, Z., Zhang, D., Zhao, G., Wang, Q., & Yang, D. (2022). The progress in titanium alloys used as biomedical implants: From the view of reactive oxygen species. *Frontiers in Bioengineering and Biotechnology*, *10*, 1092916. https://doi.org/10.3389/fbioe.2022.1092916

93. Yao, Y., & Yim, E. K. F. (2021). Fucoidan for cardiovascular application and the factors mediating its activities. *Carbohydrate Polymers*, *270*, 118347. https://doi.org/10.1016/j.carbpol.2021.118347

94. Yasin, A., Ren, Y., Li, J., Sheng, Y., Cao, C., & Zhang, K. (2022). Advances in Hyaluronic Acid for Biomedical Applications. *Frontiers in Bioengineering and Biotechnology*, *10*, 910290. https://doi.org/10.3389/fbioe.2022.910290

95. Yegappan, R., Selvaprithiviraj, V., Amirthalingam, S., & Jayakumar, R. (2018). Carrageenan based hydrogels for drug delivery, tissue engineering and wound healing. *Carbohydrate Polymers*, *198*, 385–400. https://doi.org/10.1016/j.carbpol.2018.06.086

96. Žaimis, U., Petronienė, J. J., Dzedzickis, A., & Bučinskas, V. (2023). Biodegradable Carrageenan-Based Force Sensor: An Experimental Approach. *Sensors*, *23*(23), 9423. https://doi.org/10.3390/s23239423

97. Zang, L., Zhu, H., Wang, K., Liu, Y., Yu, F., & Zhao, W. (2022). Not Just Anticoagulation—New and Old Applications of Heparin. *Molecules*, *27*(20), 6968. https://doi.org/10.3390/molecules27206968

98. Zhao, Y., Bai, J., Xue, F., Zeng, R., Wang, G., Chu, P. K., & Chu, C. (2023). Smart self-healing coatings on biomedical magnesium alloys: A review. *Smart Materials in Manufacturing*, *1*, 100022. https://doi.org/10.1016/j.smmf.2023.100022

99. Zhuang, Y., Ren, L., Zhang, S., Wei, X., Yang, K., & Dai, K. (2021). Antibacterial effect of a copper-containing titanium alloy against implant-associated infection induced by methicillin-resistant Staphylococcus aureus. *Acta Biomaterialia*, *119*, 472–484. https://doi.org/10.1016/j.actbio.2020.10.026

100. Zhuikova, Y. V., Zhuikov, V. A., Zubareva, A. A., Akhmedova, S. A., Sviridova, I. K., Sergeeva, N. S., & Varlamov, V. P. (2020). Physicochemical and biological characteristics of chitosan/κ-carrageenan thin layer-by-layer films for surface modification of nitinol. *Micron*, *138*, 102922. https://doi.org/10.1016/j.micron.2020.102922

101. Zimmerli, W., & Ochsner, P. E. (2003). Management of Infection Associated with Prosthetic Joints. *Infection*, *31*(2), 99–108. https://doi.org/10.1007/s15010-002-3079-9